Regulation of the competence to respond to stem cell self-renewal factors by Earmuff

II.Bachelors Paper

Submitted at the

Austrian Marshall Plan Foundation

Bachelor's Programme

„Medical and Pharmaceutical Biotechnology"

by
Daniel Grbac

Area of emphasis/focus/special field:

Genetic regulation of neural stem cells during development and tumorigenesis

Degree program: Medical and Pharmaceutical Biotechnology, IMC FH Krems

Internal Supervisor: Prof.(FH) DI Bernhard Klausgraber

External Supervisor: Derek Janssens

Submitted on: 19.03.2014

TABLE OF CONTENT

LIST OF FIGURES

LIST OF TABLES

ABREVIATIONS

NB	Neuroblast
INP	Intermediate neural progenitor
Imm INP	Immature intermediate neural progenitor
GMC	Ganglion mother cell
CNS	Central nervous system
MARCM	Mosaic analysis with a repressible cell marker
FLP	Flippase
FRT	Flippase recognition target
DNA	Deocyribonucleic acid
Erm	Earmuff
Dpn	Deadpan
Klu	Klumpfuss
Ase	Asense
Brat	Brain tumor
E(sp)mγ	Enhancer of split mγ
Phall	Phalloidin
UPRT	uracil phosphoribosyltransferase
UAS	Upstream activation sequence
ts	temperature-sensitive
DamID	DNA adenine methyltransferase identification
ORF	Open reading frame
PBS	Phosphate buffered saline
PBST	Phosphate buffered saline with Triton X-100
hs	heat shock
hrs	Hours
RT	Room temperature
DMF	Dimethylformamid
DEPC	Diethylpyrocarbonate
att	Attachment
ALH	After larval hatching

ABSTRACT

Stem cells have the ability to go through numerous cell cycles creating differentiated progeny but maintain at the same time an undifferentiated state through the expression of self-renewal factors. The intermediate progenitor cells often also express stem cell renewal factors but stable restriction of the developmental potential prevents them from aberrantly acquiring the stem cell-like properties. If intermediate progenitor cells possess aberrant stem cell-like properties they might serve as tumor-initiating stem cells. Thus, insight into stable restriction of the developmental potential in intermediate progenitor cells will improve the understanding of the development and the growth of tumors. As an in vivo model intermediate neural progenitors (INPs) generated by type II neural stem cells (neuroblasts) in *Drosophila* fly larval brains are used for the investigation of the mechanisms that restrict the developmental potential in INPs.

This thesis describes the restriction of the development potential of INPs to aberrantly revert into supernumerary neuroblasts (NBs) through the transcriptional repressor Earmuff (Erm). The interaction of Erm with the self-renewal factors Deadpan (Dpn), Klumpfuss (Klu), Enhancer of split (mγ (E(sp)mγ) and the BAF chromatin-remodeling complex is reported. Additionally the development of two protocols using either the TU-tagging or the TaDa-system for the further investigation of Erm function is shown. Furthermore the investigation of the novel gene CG6520 shows evidence of cooperating with Earmuff to restrict the developmental potential of INPs.

1. INTRODUCTION

Tissue-specific stem cells often use intermediate progenitor cells to generate differentiated cell types during their normal development and the maintenance of homeostasis (Chang, Wang, & Wang, 2012; Franco & Müller, 2013; Homem & Knoblich, 2012; Lui, Hansen, & Kriegstein, 2011; Ming & Song, 2011; Weng & Lee, 2011). These intermediate progenitor cells function to amplify the output of stem cells. Their development potential is restricted to prevent the intermediate progenitor cells from aberrantly acquiring stem cell like properties which as accumulating evidence suggests might be an underlying mechanism that leads to the initiation of tumoriogenesis (Haenfler, Kuang, & Lee, 2012; Liu et al., 2011; Schwitalla et al., 2013; Xiao, Komori, & Lee, 2012). Understanding how the development potential is restricted in intermediate progenitor cells may lead to novel strategies for the attenuation of tumor growth.

As an *in vivo* model the type II NB linage in *Drosophila* fly larval brains are used for the investigation of the mechanisms that restrict the developmental potential in INPs (Bello, Izergina, Caussinus, & Reichert, 2008; Bowman et al., 2008; Komori, Xiao, McCartney, & Lee, 2014; Weng, Golden, & Lee, 2010; Xiao et al., 2012). The Type II NBs can be distinguished from the other cells by their expression of Deadpan (Dpn+) and their lack of Asense (Ase-). They also divide asymmetrically to self-renew and generate a newly born INP (Fig. 1). The expression of the self-renewal factors is extinguished in the newly born imm INPs (Xiao et al., 2012) which undergo a maturation process during which their developmental potential becomes stably restricted and the expression of Ase is activated. After the maturation process the INPs start expressing the self-renewal factors again, but only divide five to six times generating exclusively differentiated progeny. This indicates that attenuating the competence to respond to NB self-renewal factors is critical for the restriction of developmental potential during the maturation of an immature INP but the mechanisms are not understood.

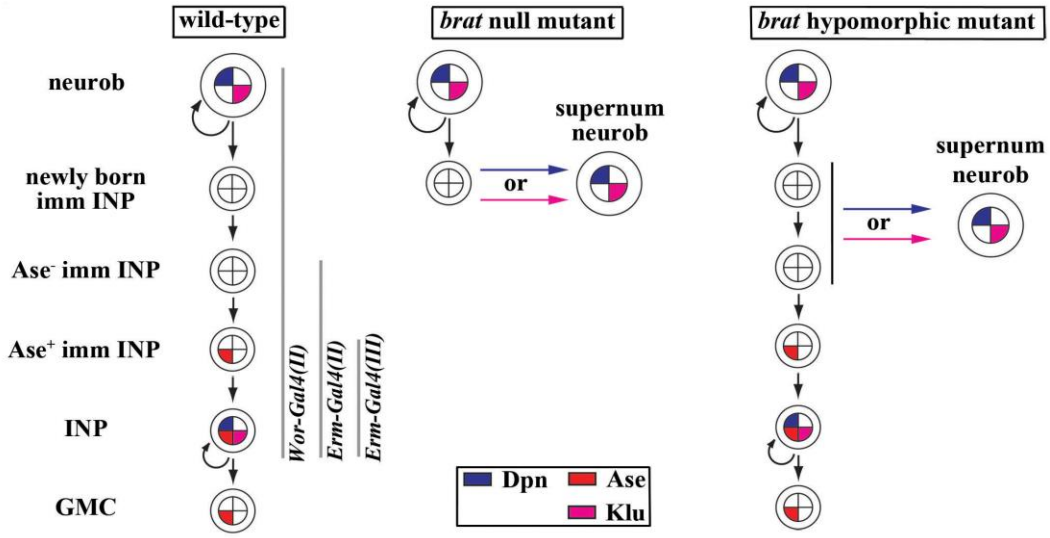

Fig 1: Type II NB linage with the brat mutant phenotype

A summary of the *brat* mutant phenotype and the expression patterns of the Gal4 drivers used to activate UAS-transgene expression at distinct stages of Type II NB linage progression (Janssens & Komori et al. 2014)

Brain tumor (Brat) and Numb are probably extinguishing the function of the self-renewal factors and thereby prevent newly born INPs from reverting into supernumerary NBs (Komori et al., 2014; Xiao et al., 2012). These self-renewal factors include Dpn, Klu, mγ (E(sp)mγ and Notch and over-expression of any of these factors throughout the type II NB lineage leads to the formation of supernumerary NBs (San-Juán & Baonza, 2011; Weng et al., 2010; Xiao et al., 2012; Zacharioudaki, Magadi, & Delidakis, 2012; Zhu et al., 2012). On the other hand, when expressing Klu and Notch in INPs only a relative mild increase in supernumerary NBs can be observed. Therefore, the INPs are functionally distinguished by NBs by the mechanisms that restrict the developmental potential in immature INPs and prevent the INPs from aberrantly reverting into NBs.

A transcription factor that distinguishes an INP from a NB is Erm (Weng et al., 2010). *erm* encodes an evolutionarily conserved C_2H_2 zinc-finger transcription factor, and the vertebrate orthologs of Erm can in a context dependent manner to activate or repress gene expression (Hirata et al., 2006; Weng et al., 2010; Yang, Dong, & Guo, 2012). For the formation of INPs Erm is not needed but in *erm* null brains the INPs spontaneously revert back into supernumerary type II NBs. However, by over-expressing *erm* or the vertebrate ortholog of *erm* (*fez* or *fezl*) the supernumerary NB phenotype is rescued which strongly suggests that Erm function is evolutionary conserved (Janssens & Komori et al. 2014).

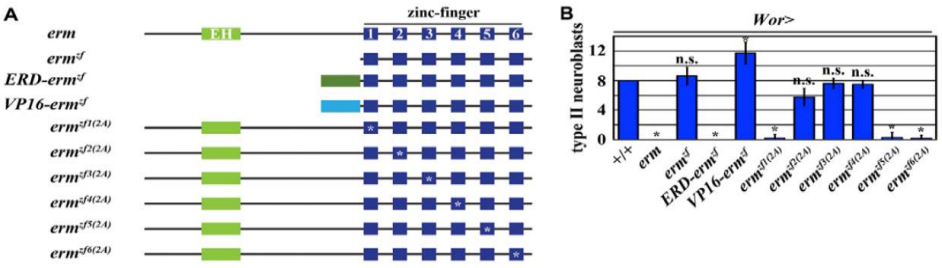

Fig 2: Schematics of erm transgenes

(A) The indicated genes were cloned into a UAS vector to investigate *erm* function. ERD, engrailed repressor domain; VP16, transactivation domain; ZF, Zink finger whereby the number besides the ZF indicates which Zink finger is mutated

(B) Quantification of total type II NBs (Dpn^+Ase^-) per brain lobe of the indicated genotypes. Numbers inside the bars indicate the number of animals used for counting. The asterisks indicate the the difference between the wt and the sample is significant while n.s. stands for non-significant. Mis-expression *of erm, ERD-erm^{zf}, erm$^{zf1(2A)}$, erm$^{zf5(2A)}$* and *erm$^{zf6(2A)}$* caused premature NB differentiation in wt brains. However, mis-expression of *erm^{zf}, erm$^{zf2(2A)}$, erm$^{zf4(2A)}$* and *erm$^{zf4(2A)}$* did not cause a significantly different phenotype compared to a wt brain. Mis-expression of *VP16-erm^{zf}* resulted in a supernumerary NB phenotype.

It was shown that Erm mainly restricts the developmental potential in the Ase^+ immature INPs. The heterozygosity of *erm* further enhances supernumerary NB formation originated from the Ase^+ immature INPs or INPs in *brat* hypomorphic brains and complete removal of *erm* function increases the frequency of supernumerary NB formation by greater than twenty-fold. However, the restoration of *erm* function in the Ase^+ immature INPs and INPs rescues the enhancement of the supernumerary NB phenotype in *brat* hypomorphic brains, and also rescues the supernumerary NB phenotype in *erm* null brains (Weng et al., 2010; Janssens & Komori et al. 2014). *UAS-erm$^{zf(2A)}$* transgenes that encode Erm transgenic proteins containing substitutions of alanine for cysteine in individual zinc-fingers were generated to observe which C_2H_2 zinc-finger elicits function of Erm in restricting developmental potential (Fig 2A). The results indicated that zinc-finger 2-4 are essential to confer Erm function as there is no significant difference in the number of NB compared to a wt brain when mis-expressing the individual zinc-finger constructs. Additionally the over expression of *UAS-VP16-erm^{zf}* resulted in an enhanced supernumerary NB phenotype indicating that it encodes a dominant-negative form of Erm (Fig 2B). Therefore it can be concluded that erm plays a critical role in the Ase^+ immature INPs or INPs to suppress supernumerary NB formation through the zinc-finger 2-4 (Janssens et al., 2014).

This thesis describes the restriction of the development potential of INPs to aberrantly revert into supernumerary NBs through the transcriptional repressor Earmuff. Erm-dependent restriction of the developmental potential in immature INPs by Erm leads to attenuated competence to respond to all known NB self-renewal factors in INPs. We also found that the Brm complex functions temporally after Brat and Numb in immature INPs. Over-expression of a dominant negative form of Brm strongly enhanced the supernumerary NB phenotype in erm hyomorphic brains. This information suggests that Erm and the Brm complex function synergistically for the stable restriction of the developmental potential in imm INPs and to functionally distinguish an INP from a NB (Janssens & Komori et al. 2014). Additionally the development of two protocols using either the TU-tagging or the TaDa system for the further investigation of Erm function is shown. We demonstrate that the novel gene CG6520 cooperates within the Erm to restrict the developmental potential of INPs, and find that it is uniquely expressed in the Central Brain in NB linages.

1.1. Control of gene expression

1.1.1. UAS-Gal4 system

The yeast positive regulatory protein GAL4 binds to four sites in the upstream activating sequence UAS to activate transcription of adjacent genes (Fig. 2A) (Giniger, Varnum, & Ptashne, 1985). This expression system can be used in *Drosophila* by inserting the GAL4 randomly into the genome, driving GAL4 expression in specific cellular subtypes genomic enhancers. By subcloning any sequence behind UAS sites a GAL4-dependent target gene can be constructed. This target gene is silent in the absence of GAL4. For activation flies carrying the target are crossed to flies expressing GAL4 resulting in their progeny expressing the target gene (Brand & Perrimon, 1993).

1.1.2. Gal80 repression

Gal80 binds to Gal4 and thereby blocks gene activation by covering the 30 amino acids at the carboxyl terminus of Gal4. These amino acids are an essential element of one of two activating regions of GAL4 (Fig. 2B) (Ma & Ptashne, 1987).

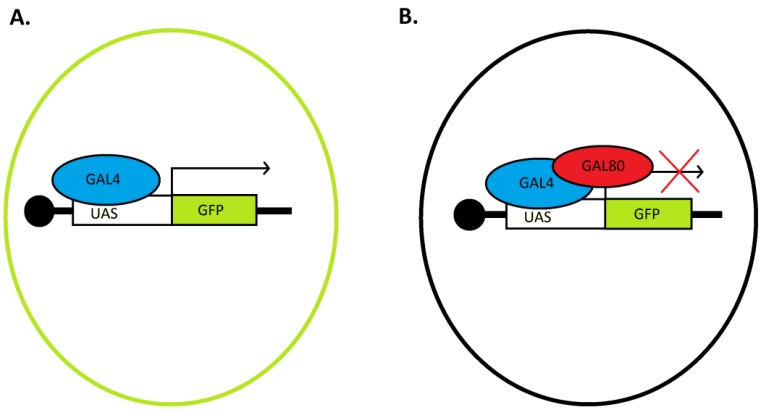

Fig. 2: GAl4 induced expression and GAL80 repression.

(A) A cell expressing GFP by Gal4 driving UAS. (B) Gal80 represses GAL4 resulting in no GFP being expressed (Wu & Luo, 2006).

Gal80 can be modified with a temperature-sensitive (ts) allele to allow temporal control over the UAS-Gal4 system in a temperature-dependent manner in *Drosophila melanogaster* (Zeidler et al., 2004).

1.2. Immunofluorescence staining

To observe the phenotypes that are created through the expression or repression of specific genes the structures or molecules specific for each cell have to be marked with fluorescence proteins to make it possible to tell them apart.

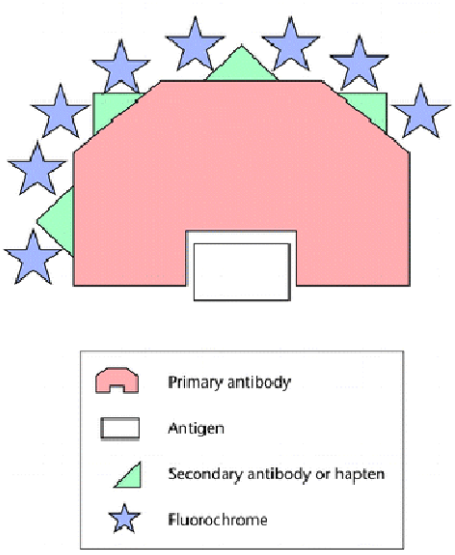

Fig. 3: Signal amplification by immunofluorescence.

The primary antibody binds to an antigen and then binds several fluorochromated secondary antibodies (Fritschy & Härtig 2001)

A widely used method to achieve this is the immunofluorescence staining. It is based on the high selectivity and affinity of antibodies for their antigens. First primary antibodies are used which bind to the target structures or molecules. These are then bound by secondary antibodies which were raised against immunoglubins of the host species used for the primaries. Hosts are the animals in which the antibodies are raised. Commonly used ones are rats, rabbits, mice and chicken. The secondary antibodies are labeled either with fluorochromes or with other haptens, which serve as anchoring sites for enzymes or fluorescent molecules, or as targets for a third antibody. As the primary antibody can bind more than one secondary antibody the signal gets stronger amplified than in other staining methods.

When staining for different targets with different fluorochromes it is necessary to choose antibodies from different hosts. The reason is that the secondary antibodies will always bind to the primary antibodies from the same species (Fritschy & Härtig 2001).

During and after staining with secondaries the brains need to be kept away from light as it would cause the fluorochromes to bleach. It is recommended to add an additional agent after staining that reduces this effect (e.g. Prolong® Gold) (Daul, Komori, & Lee, 2010).

1.3. MARCM system

In order to visualize single cell lineages in the developing brain, and also to investigate the molecular mechanisms underlying the observed phenomena, a genetic system for performing mosaic analysis in the *Drosophila* CNS is used. This involves the generation of homozygous mutant cells from heterozygous precursors using mitotic recombination. Since for most genes one wild-type allele in a diploid cell is sufficient for normal gene function it can be knocked out in a small subset of cells by creating homozygous mutant cells in heterozygous tissues. Thereby their phenotypes can be observed in an otherwise phenotypically wild-type organism (T. Lee & Luo, 2001).

Therefore the Mosaic analysis with repressible cell marker (MARCM) system is used to allow labeling of homozygous mutant cells uniquely in mosaic tissues (T. Lee & Luo, 2001). The system uses the FLP/FRT system of the 2µm plasmid of the yeast Saccharomyces cerevisiae. The recombinase FLP acts on copies of the recombination target FRT which results in the inversion of one section of the plasmid relative to the other (Golic & Lindquist, 1989).

To create a situation in which only mutated cells are labeled the marker is placed under the control of the repressible promoter and a transgene is introduced to allow ubiquitous expression of the repressor. By placing the repressor transgene distal to the FRT site in trans to the mutant chromosome arm only cells homozygous for the mutation will lack the repressor transgene. Since the repressor is preventing expression of the marker in the other cells only the cell homozygous for the mutation will be stained. To achieve this the UAS-Gal4 system and its repressor Gal80 are used (T. Lee & Luo, 1999).

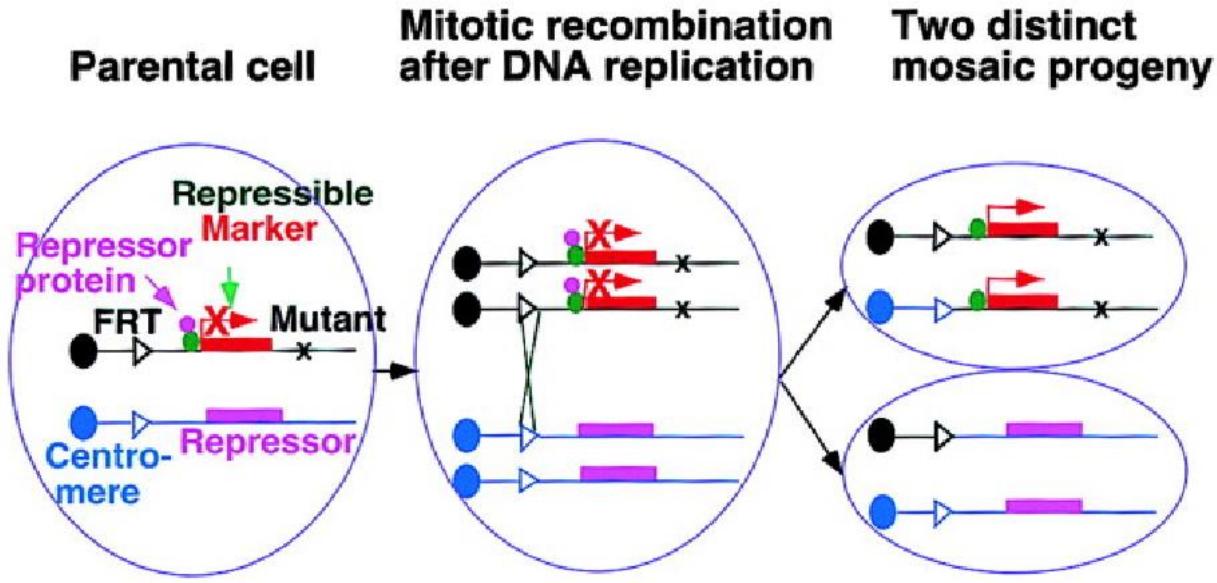

Fig 3: Mitotic recombination in the MARCM system.

A transgene encoding the repressor of marker gene expression is placed distal to the FRT site on the homologous chromosome arm from the mutant gene. The marker gene can be only expressed in homozygous mutant cells due to the loss of the repressor transgene (T. Lee & Luo, 1999).

1.4. TU-tagging system

The TU-tagging system was developed to enable the isolation of cell type specific RNA from intact complex tissues (Miller, Robinson, Cleary, & Doe, 2009).

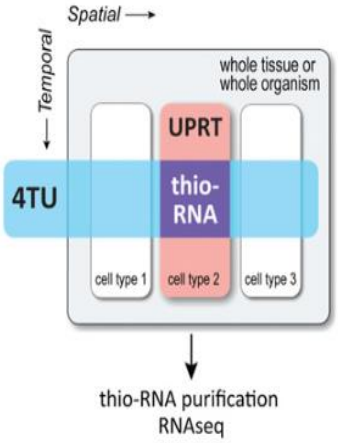

Fig 4: Schematic of the TU tagging method

Spatial control was provided by cell type-specific expression of UPRT (red), and temporal control was achieved by a pulse of 4TU (blue). Only UPRT^{+} cells exposed to 4TU will generate thio-labeled newly transcribed RNA, which then can be purified from the intact tissue or organism (Gay et al., 2013).

The system uses the Toxoplasma gondii nucleotide salvage enzyme uracil phosphoribosyltransferase (UPRT) which can be used to biosynthetically label newly synthesized RNA in vivo (Cleary, Meiering, Jan, Guymon, & Boothroyd, 2005; Miller et al., 2009). UPRT couples ribose-5-phosphate to the N1 nitrogen of uracil to yield

uridine monophosphate which is then incorporated into RNA. By providing the modified uracil analog 4-thiouracil (4TU) to UPRT as a substrate the product will be incorporated into the RNA. This incorporation has fortunately little effect of cellular physiology. The thio-labeled RNA can then be readily tagged and purified using commercially available reagents (Fig. 4)(Cleary et al., 2005; Miller et al., 2009).

We worked on developing a protocol to use the UPRT system to observe gene expression changes specifically in *erm* mutant immature INPs and reverted NB.

1.5. TaDa system

The TaDa system was developed to asses genome-wide protein binding *in vivo* in a cell type-specific way without using cell purification (Southall et al., 2013). This system is based on DNA adenine methyltransferase identification (DamID) (van Steensel, Delrow, & Henikoff, 2001; van Steensel & Henikoff, 2000). It fuses an Eschericha coli DNA adenine methyltransferase to a DNA- or chromatin-binding protein of interest. The fusion proteins biding site is tagged by adenine methylation when expressed but if Dam is expressed at high levels it is toxic and can lead to nonspecific methylation (van Steensel & Henikoff, 2000).

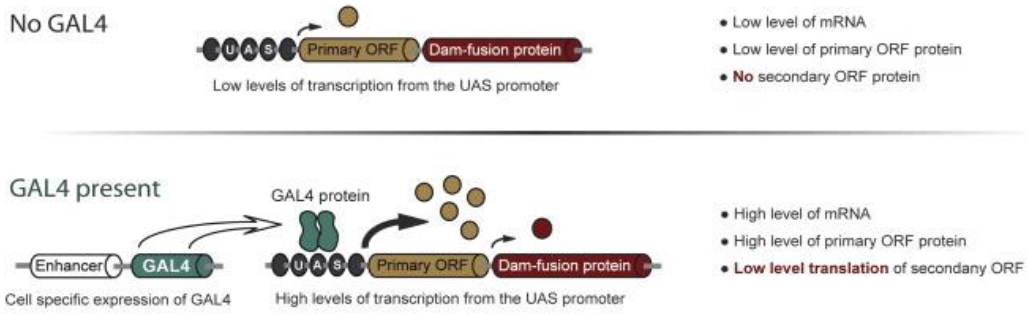

Fig 5: Schematic representation of the TaDa method.

Translation of the Dam-fusion protein is greatly reduced by the addition of an upstream ORF and by ribosome re-initiation. This prevents expression of the Dam-fusion in uninduced cells and nonspecific methylation in induced cells (Southall et al., 2013).

Thus DamID requires the methylase-fusion protein to be expressed at extremely low levels. This can be achieved by driving transgene expression exclusively from a basal promoter, but the downside is that the Dam-fusion protein is then expressed constitutively in all cell types (Bianchi-Frias et al., 2004; Choksi et al., 2006; Vogel,

Peric-Hupkes, & van Steensel, 2007). Therefore the TaDa system uses Gal4 to drive expression and the transgene UAS-LT3-Dam ORF1 which also encodes full-length mCherry (Shaner et al., 2004; Southall et al., 2013). This allows nontoxic expression at any stage of development and has the additional advantage of marking the expressing cells with mCherry (Southall et al., 2013).

1.6. Gateway cloning

This technology is based on the bacteriophage lambda site-specific recombination system which facilitates the integration of lambda into the E.coli chromosome (Guarante, Roberts, & Ptashne, 1992). The components of the lambda recombination sytem are modified to improve specificity and efficiency of the system (Bushman, Thompson, Vargas, & Landy, 1985).

The recombination occurs between specific attachment (att) sites on the interacting DNA molecules and is conservative without requiring DNA synthesis. The sites are attB on the E.coli chromosome and attP on the lambda chromosome (Weisberg, Enquist, Foeller, & Landy, 1983). Upon lambda integration recombination occurs between attB and attP sites to give rise to attL and attR sites (Landy, 1989).

The lambda recombination is catalyzed by an enzyme mixture. The enzymes bind to specific sequences, bring together the target sites, cleave them and covalently attach the DNA. The recombinational proteins involved in the reaction are E.coli Integration Host Factor proteins in the lysogenic pathway and Excisionase proteins + E.coli Integration Host Factor proteins in the lytic pathway. Both ways use bacteriophage λ Integrase (Landy, 1989).

The Gateway technology uses the lambda recombination to facilitate transfer of heterologous DNA sequences between vectors (Hartley, Temple, & Brasch, 2000). Two reactions are the basis of the Gateway technology. The first one is the BP reaction which facilitates recombination of an attB substrate with an attP substrate to create an attL-containing entry clone. The second one is the LR reaction which facilitates recombination of an attL substrate with an attR substrate to create an attB containing expression clone (The Gateway® Technology manual).

2. MATERIALS & METHODES

2.1. Fly strains

Mutant and transgenic fly strains used include *erm*^{1}, *erm*^{2} and *UAS-erm-HA* (Weng et al., 2010), *klu*^{R51} (Kaspar, Schneider, Chia, & Klein, 2008), *UAS-klu-HA* (Xiao et al., 2012), *dpn*^{1} (Younger-Shepherd, Vaessin, Bier, Jan, & Jan, 1992), *Erm-GAL4(II)* and *Erm-GAL4(III)* (Pfeiffer et al., 2008), *Wor-GAL4* (C.-Y. Lee, Robinson, & Doe, 2006), *UAS-brat-myc* (Xiao et al., 2012), *UAS-dpn* (Wallace, Liu, & Vaessin, 2000). The following fly stocks were obtained from the Bloomington *Drosophila* Stock Center: Oregon R, *brat*^{DG19310} (Xiao et al., 2012), , *tub-GAL80, UAS-mCD8-GFP, FRTG13, FRT2A and hs-flp* (T. Lee & Luo, 2001), *tub-GAL80*^{ts} (McGuire, Le, Osborn, Matsumoto, & Davis, 2003), *Elav-GAL4*. The additional transgenic fly strains used for the isolation protocols include UAS-UPRT (Cleary et al., 2005; Miller et al., 2009), LT3-PolII (Southall et al., 2013)

2.2. Clonal analysis

MARCM clones were induced 24hrs after larval hatching (ALH) by a 90 minutes heat shock at 38^{o}C (Janssens & Komori et al. 2014).

To examine *klu*^{R51} mutant clones in an *erm* mutant background either (1) *erm*^{1},*hs-flp/ CyO*,*Act5C-GFP*; *FRT2A,Wor-GAL4,* or (2) *erm*^{1}*,hs-flp/ CyO*,*Act5C-GFP*; *klu*^{R51}*,FRT2A,Wor-GAL4/ TM6B,Tb* virgin females were crossed to either (3) *UAS-mCD8-GFP*; *Tub-Gal80,FRT2A*, or (4) *erm*^{2},*UAS-mCD8-GFP*/*CyO*,*Act5C-GFP; Tub-Gal80,FRT2A* males (Janssens & Komori et al. 2014).

To examine *dpn*^{1} mutant clones in an *erm* mutant background, *Elav-GAL4*,*UAS-mCD8-GFP,hs-flp; erm*^{1}*,FRTG13,TubGAL80/CyO,Act5C-GFP* virgin females were crossed to either (1) *FRTG13,* (2) *FRTG13,dpn*^{1}*/ CyO,Act5C-GFP* (3) *erm*^{2}*,FRTG13/CyO,Act5C-GFP,* or *(4) erm*^{2}*,FRTG13,dpn*^{1}*/CyO,Act5C-GFP* males (Janssens & Komori et al. 2014).

For overexpression studies larvae were collected at 0-4hrs ALH raised at 31^{o}C and dissected at 72hrs ALH (Janssens & Komori et al. 2014).

2.3. Immunofluorescence staining and antibodies

Larval brains were dissected in 1X PBS solution. Larval brains were fixed in 4% formaldehyde in 1XPBS containing 0.3% Triton X-100 (PBST) for 24 minutes and processed for immunofluorescent staining according to a previously published protocol (Weng, Komori, & Lee, 2012). Antibodies used in this study include rat anti-Dpn (1:1000) (Xiao et al., 2012) , rat anti-Wor (1:1) (C.-Y. Lee, Robinson, et al., 2006), rabbit anti-Ase (1:400) (Weng et al., 2010), mouse anti-Pros (MR1A, 1:100) (C.-Y. Lee, Wilkinson, Siegrist, Wharton, & Doe, 2006), mouse anti Elav (1:100; 9F8A9, DSHB), mouse anti-Dlg (1:50; 4F3E3E9, DSHB), chicken anti-GFP (1:2000; cat # 1020, Aves Labs), chicken anti-β-Gal (1:2000; cat# 1040, Aves Labs), and rabbit anti-RFP (1:100; cat# 600-401-379, lot# 25003, Rockland). Secondary antibodies were from Molecular Probes and Jackson Labs (details are available upon request). We used Rhodamine phalloidin (1:100; Invitrogen) to visualize cortical actin. The confocal images were acquired on a Leica SP5 scanning confocal microscope (Janssens et al., 2014).

2.4. Protocol for isolation of specific RNA using the TU-tagging system

To enrich the desired RNA sample for relevant erm target genes UAS-UPRT and UAS-erm were co-overexpressed within $erm^{1/2}$ mutant type II NB linages. Additionally tub-$Gal80^{ts}$ was combined with Ase-Gal80 and wornui-Gal4 or Ase-Gal4 to temporally and spatially control the expression of transgenes within the type II NB linages. By comparing the transcriptional profiles between Type I and Type II NB linages we hope to identify novel transcriptional programs that distinguish stem cell types.

All experiments were conducted in an RNAse free environment.

To supply the 4TU to the larva TU-food was made up combining the ingredients from Tbl. 2 which were added to Dimethylsulfoxid (DMSO) to reach the final desired volume. Thereby it was important to first mix only the 4TU with the solution, heat it in a microwave to dissolve it properly and add the oxalic acid only after the temperature of the mixture has dropped below 60°C.

Tbl. 1: Ingredients for TU-food

	concentration	Amount for 200ml food
4TU	0.5mM	0.0098g
Oxalic acid	1mM	0.039g

Larvae containing the combination of transgenes were grown at 25°C on standard meal caps for 72 hrs. and then transferred to the TU-food and shifted to 31°C for additional 5-8 hrs. to induce transgene expression. The larval brains were then harvested. The amount of larvae was chosen so that about 500 brains can be gained. 20 brains were put into a well containing PBS which was then removed and replaced by 50µl Trisol. The sample was then snap frozen before the next well was filled with brains to ensure that no cell death processes occur in the brains.

2.4.1. Trisol treatment

The tissue was homogenized using a glass homogenizer. Then the insoluble material was removed by spinning the tubes at 12000 x g for 10 min. at 4°C and transferring the Trisol solution into a new microfuge tube. After leaving them for 5 min incubating at RT 0.2 ml Chloroform per 1 ml Trisol was added. The solutions were then mixed by shaking vigorously for 15 sec and then incubated for 3 min at RT. After centrifuging at 10,000 x g for 15 min at 4°C the mixture separated into 3 phases. The upper phase was transferred to a fresh microfuge tube and the rest discarded. Isopropanol was added (amount = ½ volume original Trisol) and then the solutions were incubated for 10 min at RT. The tubes were then centrifuged at 10,000 x g for 10 min at 4°C resulting in a pellet at the bottom of the tubes. The supernatant was removed and the pellet washed with 1 ml Ethanol. After mixing by vortexing the tubes were centrifuged at 7,500 x g for 5 min at 4°C. Next the Ethanol was removed and the pellet left to air dry for about 5 min. The RNA was resuspended in 50 µl RNase free water and then the concentration was measured using a nanodrop machine. If the A 260/280 was <2 a RNA cleanup was performed using the RNeasy MinElute Cleanup Kit according to the RNeasy MinElute Cleanup Handbook. The final RNA yield should be >30 µg.

2.4.2. Biotinylation of TU-RNA

The RNA was diluted to a concentration of 0.15 µg/µl using RNase free water and the Biotinylation mix was prepared (Tbl. 3).

Tbl. 2: Biotinylation mix

RNA (0.15 µg/µl) in RNase free water	350 µl
10 x Biotinylation Buffer (100 mM Tris pH 7.4 + 10 mM EDTA)	50 µl
Biotin HPDP (1 mg/ml DMF)	100 µl
	500 µl

The mix was mixed by pipetting and then incubated at RT for 1.5 hrs on a rotor. Next 500 µl Chloroform/Isoamylalcohol (24:1) were added and mixed by shaking. After incubating for 3 min at RT the solutions were centrifuged at 20,000 x g for 5 min at RT. The upper phase was transferred to a phaselog gel tube which was centrifuged before at 16,000 x g for 30 sec. A volume of Chloroform/Isoamylalcohol (24:1) equal to the solution was added and then the tubes were shaken vigorously to mix. After incubating for 3 min at RT the tubes were centrifuged at 16,000 x g for 5 min at RT. The upper aqueous phase was transferred to a fresh microfuge tube.

2.4.3. RNA precipitation

A volume of 5 M NaCl equal to 1/10 of the reaction volume as well as a volume of isopropanol equal to the resulting volume were added. After mixing by shaking vigorously the tubes were centrifuged at 20,000 x g for 20 min at 4°C. Then the supernatant was removed and the pellet washed using 500 µl 75% Ethanol and mixing by vortexing. Next the solutions were centrifuged at 20,000 x g for 10 min at 4°C and the resulting supernatant was removed. After air-drying the pellet for 5 min it was resuspended in 50 µl RNase free water.

2.4.4. Purification of biotinylated TU-RNA

The biotinylated RNA as well as the washing buffer (100 mM Tris pH 7.4 + 10 mM EDTA + 1 M NaCl + 0.1% Tween 20) were heated to 65°C for 10 min. The RNA was then placed on ice for 5 min and then 100 µl streptavidin beads were added. After incubating the solution for 15 min at RT µMacs columns were placed on a magnetic stand. 900 µl washing buffer was added to each and allowed to flow through to equilibrate the columns. The biotinylated RNA with the beads was then applied to the columns. After letting the solutions sink into the columns the columns were washed 3 times with 900 µl of 65°C washing buffer and then 3 x with 900 µl RT washing buffer. Then the elution buffer was prepared (Tbl. 4) as well as 2 ml tubes containing 700 µl Buffer RLT (RNeasy MinElute Cleanup Kit Handbook) which were placed underneath the columns. The RNA was eluted into the tubes by letting 2 x 100 µl elution buffer flow through the column. The RNA was then treated using the RNeasy MinElute Cleanup Kit (RNeasy MinElute Cleanup Kit Handbook). For the resuspension of the final pellets 15 µl RNase free water was added to each.

Tbl. 3: elution buffer mix

β- Mercaptoethanol	10 µl
RNase free water	190 µl

2.4.5. Troubleshooting

For troubleshooting purposes UAS-UPRT fly strains from the Cleary lab, the O'connor lab and tub-Gal4 were crossed to hs-Gal4. The tub and hs promoters were used to drive expression constitutively in all cell type, reducing the number of animals we had to dissect in order to get a suitable amount of RNA for an experiment.

2.5. Protocol for isolation of specific DNA using the TaDa system

2.5.1. Genomic DNA isolation (Qiagen DNeasy Blood and Tissue Kit)

100 brains were dissected into 180 µl Buffer ATL (Qiagen DNeasy Blood and Tissue Kit) and then 20 µl proteinase K + 20 µl RNaseA (about 40 µg) were added. The solutions are mixed through inverting several times and then were incubated at 56°C until the tissue was completely lysed (1-3 hrs). Next 200 µl Buffer AL (Qiagen DNeasy Blood and Tissue Kit) was added to the sample and mixed immediately by pipetting up and down gently (50x). Then 200 µl Ethanol (100%) was added and mixed again by pipetting. The solution was applied to a spin column and spun at 8,000 rpm for 1 min. After discarding the flow through 500 µl AW1 (Qiagen DNeasy Blood and Tissue Kit) was added and spun at 8,000 rpm for 1 min. The flow through was discarded and 500 µl AW2 (Qiagen DNeasy Blood and Tissue Kit) was added to the column which was then spun at 13,000 rpm for 3 min. After discarding the flow through the spin column was placed into a 1.5 microfuge tube and 200 µl AE (Qiagen DNeasy Blood and Tissue Kit) buffer was added. Then the solution was left for incubation at RT for 30 min and spun at 8,000 rpm for 1 min. The flow through was kept and the spin column placed into a new microfuge tube which was then filled with 200 µl AE buffer (Qiagen DNeasy Blood and Tissue Kit). After a 10 min incubation at RT the flow throughs were combined and 2 µl gDNA from the elution was run on a 0.7% agarose gel. Then the concentration was measured using a nanodrop machine.

2.5.2. Genomic DNA precipitation

The gDNA was mixed with MilliQ water to get 3 µg DNA in a total volume of 400 µl. Next 800 µl 100% Ethanol, 40 µl 3 M Sodium Acetate (pH 5.2) and 2 µl molecular biology grade glycogen are added. After mixing by inverting the samples are incubated at -20°C for 20 min and spun at 13,000 rpm for 30 min at 4°C. The supernatant was then removed and 500 µl 70% Ethanol was added to each pellet. The tubes were spun at 13,000 rpm for 10 min at 4°C and then the Ethanol was removed. The pellet was left to dry for 5 min.

2.5.3. DpnI digestion

10 µl DpnI master mix (Tbl. 5) was added directly on the dried pellet and then incubated at RT for 30 min to allow the pellet to resuspend. The digest was transferred to a PCR tube and incubated at 37°C over night. Next 0.5 µl DpnI enzyme was added and incubated at 37°C for 1 hour. After incubating at 80°C for 20 min the solutions were cooled down to 4°C. For the control 1.0 µl DEPC water was added instead of the DpnI enzyme.

Tbl. 4: DpnI master mix

Buffer 4 (10x, NEB)	1.0 µl
DEPC water	8.0 µl
DpnI (20 U/µl, NEB)	1.0 µl

2.5.4. Ligation

The ligation master mix (Tbl. 6) was prepared and 5 µl DpnI digested gDNA were transferred to PCR tubes. 15 µl ligation master mix was added to each and the PCR machine was programmed to ligate at 16°C for 2 hrs. followed by 65°C for 10 min to inactivate the ligase. For the control 1.0 µl DEPC water was added instead of the T4 quick ligase.

Tbl. 5: ligation master mix

10x ligation buffer (NEB)	2.0 µl
Ds-AdR	0.8 µl
DEPC water	11.2 µl
T4 quick ligase (5 U/µl, NEB)	1.0 µl

2.5.5. DpnII digestion

60 µl DpnII digestion master mix (DpnII master mix) were added to the 20 µl ligated DNA and then left for digestion at 37°C for 1 hour.

Tbl. 6: DpnII master mix

DpnII buffer (10x, NEB)	8.0 µl
Dpn II (10 U/µl, NEB)	1.0 µl
DEPC water	51.0 µl

2.5.6. PCR amplification

60 µl PCR master mix (Tbl. 8) was added to the DpnII digested gDNA and the solution was split into 2 x 40 µl reactions in PCR strips.

Tbl. 7: PCR master mix

10x cDNA PCR reaction buffer (Clontech)	8.0 µl
AdR-PCR primer (50 uM)	1.25 µl
50x dNTP mix (Clontech)	1.6 µl
Advantage DNA polymerase mix (50X, Clontech)	1 µl
DEPC water	48.15 µl

Next the PCR was run according to Tbl. 9. 3 µl PCR product was run on a gel to check the quality. The QUIAGEN PCR purification kit (150 µl PCR product + 750 µl Buffer PB) was used to purify the product. Then 32 µl DEPC water was added for elution and incubated at RT for 15 min. The samples were diluted to a concentration of 2 µl DNA in 10 µl DEPC water.

Tbl. 8: PCR programm

Temp.	Time
68°C	10 min
94°C	30 sec
65°C	5 min
68°C	15 min
Repeat 3x	
94°C	30 sec
65°C	1 min
68°C	10 min
Repeat 17x	
94°C	30 sec
65°C	1 min
68°C	2 min
4°C	Hold

2.6. Cloning of CG6520 promoter

To shuttle the CG6520 promoter into the desired pBPG Gal4 expression vector the Gateway Technology was used (Liang, Peng, Baek, & Katzen, 2013). The CG6520 promoter region was amplified from a fly's genome using PCR with Primers specially designed for this purpose. After running the sample on a gel the CG6520 promoter was cut out of the gel. Then a gel extraction was performed according to the QIAquick Gel Extraction Kit Handbook using the QIAquick Gel Extraction Kit. The PCR product was then cloned into pENTR/D-TOPO. Using a direction TOPO reaction, 3 colonies were grown up and a Restriction Digest was performed to test which colonies contained the insert. One of the cell colonies that had the insert was then picked to be used as the entry clone. This entry clone was then transferred into the destination vector pBPG using a LR reaction. The LR reaction mix was made up (Tbl. 11) and mixed by vortexing twice for 2 sec. After the sample was incubated at 25°C for 60 min 2 µl proteinase K was added and incubated for 10 min at 37°C. 1 µl of the LR reaction solution was used to perform another competent cell transformation. The resulting colonies were then checked for the insert using PCR amplification and gel electrophoresis (Gateway® Technology manual). Cells containing the insert were then sent to the company Bestgene which performed fly injections and send back flies containing the CG6520 promoter region driving Gal4.

Tbl. 9: BP reaction mix (Gateway® Technology manual)

Component	Amount
PCR product (40-100 fmol)	3 µl
pENTR/D-TOPO (150 ng/µl)	2 µl
TE Buffer, pH 8.0	7 µl

Tbl. 10: LR reaction mix (Gateway® Technology manual)

Component	Amount
Entry clone (100-300 ng/ reaction)	3 µl
Destination vector (300 ng/ reaction)	2 µl
5X LR Clonase Reaction Buffer	4 µl
TE Buffer, pH 8.0	7 µl
LR Clonase™ enzyme mix	4 µl

3. RESULTS

3.1. Erm restricts the developmental potential in immature INPs leading to attenuated competence to respond to Klu in INPs

It was observed that over-expression of *erm* from Ase^{-} immature INPs efficiently suppressed supernumerary NB formation in *brat*$^{DG19310/11}$ brains, but over-expression of *erm* from Ase^{+} immature INPs could not (Fig 6A-C). These results lead to the conclusion that *brat* as well as *erm* suppress supernumerary NB formation by regulating similar downstream mechanisms. There is evidence that brat suppresses supernumerary NB formation by antagonizing *klu* (Xiao et al., 2012). The miss-expression of *klu* from Ase^{-} immature INPs in *brat*$^{DG19310/11}$ brains led to supernumerary NB formation, mis-expression of *klu* from Ase^{+} immature INPs had no effect (Fig. 6H). Therefore it was hypothesized that *erm* restricts developmental potential by antagonizing *klu* function. Through miss-expression of *klu* from Ase^{-} immature INPs in wild-type brains it could be observed that by co-expressing erm the resulting supernumerary NB formation was completely suppressed (Fig. 6D-E, H). Erm target genes can act cooperatively with Klu to promote a NB fate as seen by the mis-expression of *VP16-erm*^{zf} or *klu* alone from Ase^{+} immature INPs not having any effect but the co-expression of *VP16-erm*^{zf} and klu inducing supernumerary NB formation (Fig 6H). Also in erm hypomorphic brains the supernumerary NB formation was enhanced by mis-expression of klu from Ase+ immature INPs (Fig 6F-H) (Janssens & Komori et al. 2014).

The suppression of supernumerary NB formationin *erm* null brains by removing *klu* function was tested by observing GFP-marked mosaic clones derived from a single type II NB in *erm* null brains. These clones contained multiple NBs per clone (Fig. 6I). Clonally removing klu function strongly suppressed supernumerary NBs in *erm* null brains (Fig. 6I) (Janssens & Komori et al. 2014).

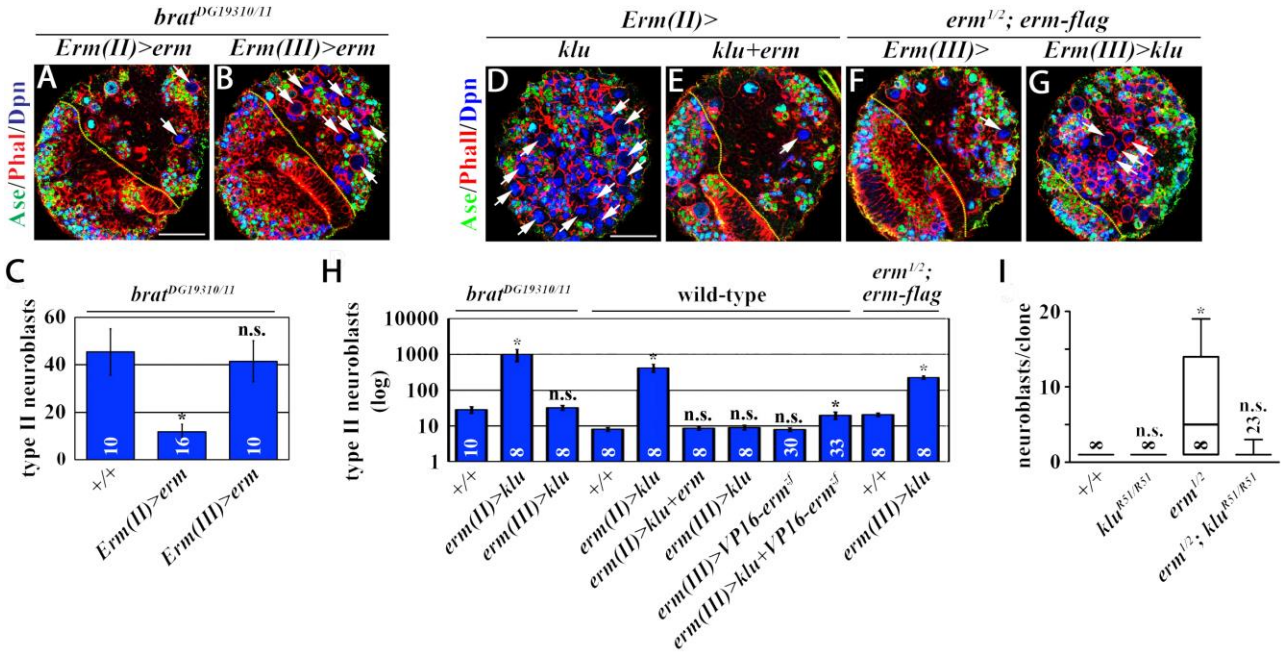

Fig 6: Erm-dependent restriction of developmental potential in immature INPs leads to attenuated competence to respond to Klu in INPs (Janssens & Komori et al. 2014)

(**A-C**) Over-expression of erm in Ase$^-$ immature INPs can suppress the supernumerary NB phenotype in brat hypomorphic brains. (A-B) Third instar larval brains of the indicated genotypes were stained for the markers indicated. Scale bar, 40 µm. (C) Quantification of total type II NBs (Dpn$^+$Ase$^-$) per brain lobe of the indicated genotypes. Numbers inside the bars indicate the number of animals used for counting. The asterisks indicate the the difference between the wt and the sample is significant while n.s. stands for non-significant.

(D-H) Co-expression of erm can suppress the supernumerary NB phenotype induced by mis-expression of klu. (D-G) Third instar larval brains of the indicated genotypes were stained for Dpn, Ase and Phall. Scale bar, 40 µm. (H) Quantification of total type II NB (Dpn$^+$Ase$^-$) per brain lobe of the indicated genotypes.

(**I**) Removal of klu function suppresses supernumerary NB formation in erm null brains. Quantification of total type II NBs (Dpn$^+$Ase$^-$) per clone for the indicated genotypes.

3.2. Erm restricts developmental potential in immature INPs by attenuating the competence to respond to Dpn and E(spl)mγ in INPs

The miss-expression of *dpn* from Ase^{+} immature INPs led to a significantly milder supernumerary NB phenotype in *brat*$^{DG19310/11}$ brains than from Ase^{-} immature INPs (Fig. 7A, Fig. 8A-C). In wild type brains the co-expression of *erm* completely suppressed supernumerary formation induced by mis-expression of *dpn* from Ase^{-} immature INPs (Fig. 7A-C). Also co-expression of *VP16-erm*^{zf} and *dpn* from Ase^{+} immature INPs led to a significant increase in supernumerary NB as compared to mis-expression of *dpn* alone under the identical conditions (Fig. 7A). In erm hypomorphic brains the mis-expression of *dpn* in Ase^{+} immature INPs enhanced supernumerary NB formation (Fig. 7A, D-E). Furthermor, by clonally removing the function of *dpn* strongly suppressed the supernumerary NB phenotype in *erm* null brains (Fig. 7F) (Janssens & Komori et al. 2014).

Simmilar to *dpn* mis-expression of *E(spl)mγ* from Ase^{+} immature INPs led to a significantly milder supernumerary NB phenotype in *brat*$^{DG19310/11}$ brains than from Ase^{-} immature INPs (Fig. 7G). Also the co-expression of *erm* strongly suppressed supernumerary formation induced by mis-expression of *E(spl)mγ* in Ase^{-} immature INPs in wild-type brains (Fig. 7G). The mis-expression of *E(spl)mγ* alone from Ase^{+} immature INPs did not have any effect, however the co-expression of *VP16-erm*^{zf} and *E(spl)mγ* induced supernumerary NBs (Fig. 7G). Furthermore, mis-expression of *E(spl)mγ* from Ase^{+} immature INPs enhanced supernumerary NB formation in *erm* hypomorphic brains (Fig. 7G) (Janssens & Komori et al. 2014).

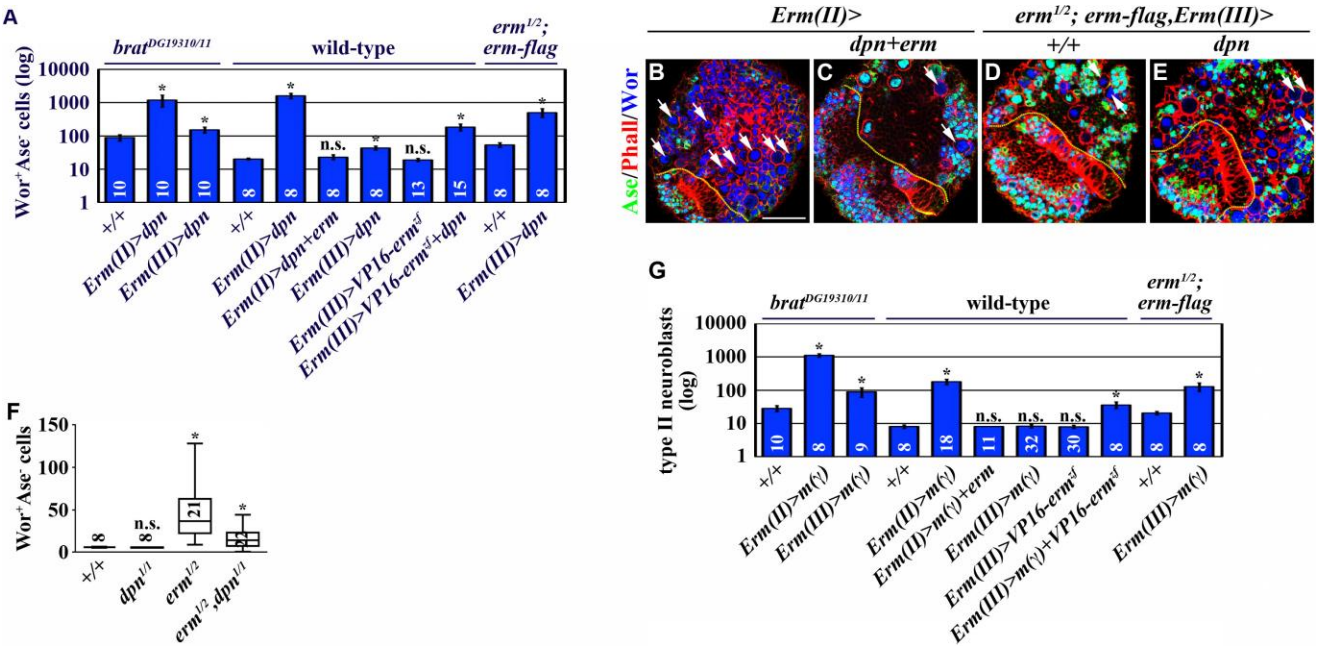

Fig 7: Erm-dependent restriction of developmental potential in immature INPs leads to attenuated competence to respond to Dpn and E(spl)mγ in INPs (Janssens & Komori et al. 2014)

(A-E) Co-expression of *erm* can suppress the supernumerary NB phenotype induced by mis-expression of *dpn*. Quantification of total Wor^{+}Ase^{-} cells (including type II NBs and Ase- immature INPs) per brain lobe of the indicated genotypes. (B-E) Third instar larval brains of the indicated genotypes were stained for Wor, Ase and Phall. Scale bar, 40 µm.

(F) Removing *dpn* function suppresses supernumerary NBformation in erm null brains. Third instar larval brains carrying GFP-marked mosaic clones derived single NBs of the indicated genotypes were stained for GFP, Wor, Ase, Pros and Elav. Quantification of total Wor^{+}Ase^{-} cells (including type II NBs and Ase^{-} immature INPs) per clone for the indicated genotypes.

(G) Mis-expression of *E(spl)mγ* from Ase^{+} immature INPs led to a significantly milder supernumerary NB phenotype in *bratDG$^{19310/11}$* brains than from Ase^{-} immature INPs. Quantification of total type II NBs (Dpn^{+}Ase^{-}) per brain lobe of the indicated genotypes. Numbers inside the bars indicate the number of animals used for counting. The asterisks indicate the the difference between the wt and the sample is significant while n.s. stands for non-significant.

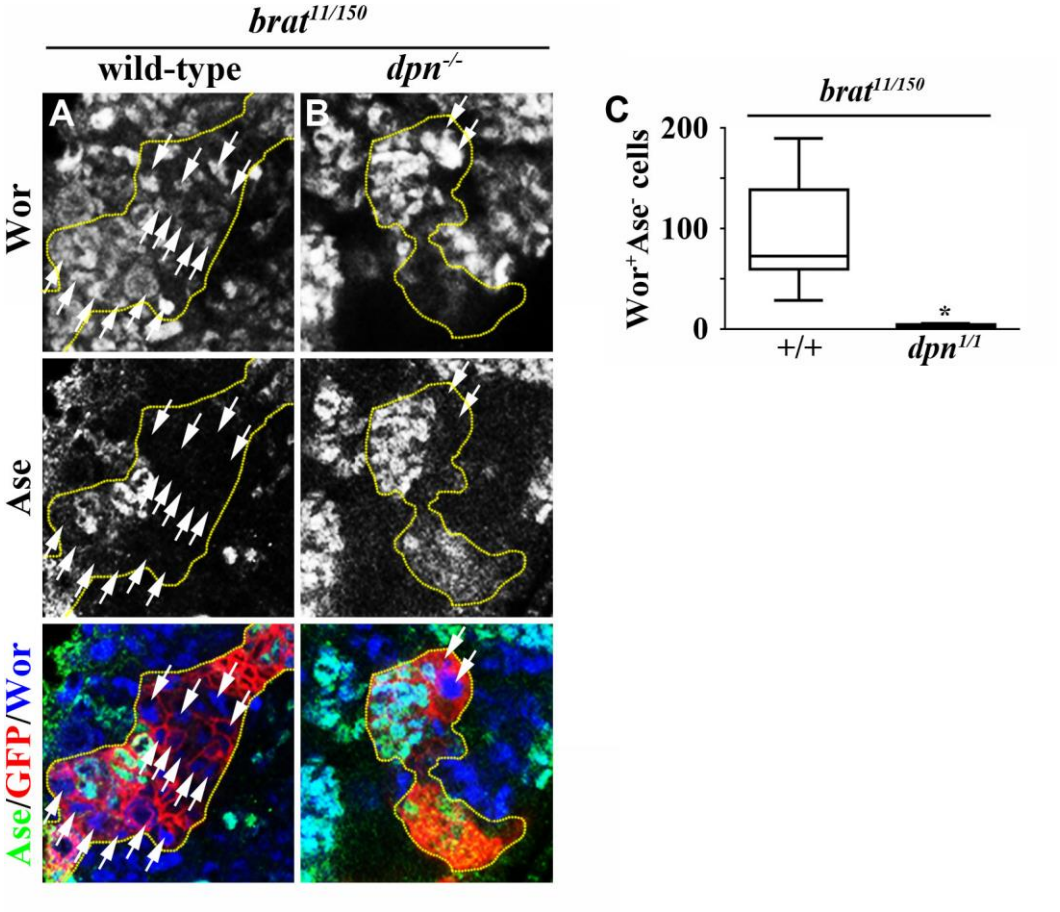

Fig 8: Dpn causes formation of supernumerary NBs in brat null bains (Janssens & Komori et al. 2014).

(A-C) Removing *dpn* function in *brat* null brains reduces the supernumerary NB phenotype. (A-B) Third instar larval brains carrying GFP-marked mosaic clones derived single NBs of the indicated genotypes were stained for GFP, Ase and Wor. (C) Quantification of total $Wor^{+}Ase^{-}$ cells (including type II NBs and Ase^{-} immature INPs) per clone for the indicated genotypes.

3.3. The Brm complex suppresses supernumerary neuroblast formation by preventing the developmental potential in immature INPs

It was observed that the *brm, mor* and *osa* genes act as genetic enhancers of *brat*. The heterozygosity of any of these three genes enhanced the supernumerary NB phenotype in $brat^{DG19310/11}$ brains while having no effects on type II NB linages in wt brains(Fig. 9A-E). Since *brm, mor* and *osa* encode the core components of the BAF chromatin-remodeling complex (Carrera, Zavadil, & Treisman, 2008; Mohrmann et al., 2004), it was hypothesized that the BAF complex functions in immature INPs to suppress supernumerary NB formation. Also by over-expressing the dominant negative form of Brm, the transgene $UAS\text{-}brm^{DN}$, throughout the type II linage or specifically in Ase^{-} immature INPs enhanced the supernumerary NB phenotype in $brat^{DG19310/11}$ brains (Fig. 9F-I) (Janssens & Komori et al. 2014).

Next it was tested whether the BAF complex also functions temporally after Numb to suppress supernumerary NB formation. Since a numb null type II NB clone containing more than one hundred supernumerary NB and newly born immature INPs, were it normally functions, is too severe for testing gene function in immature INPs (Xiao et al., 2012), $numb^{NP2301/15}$ was used instead. Brain lobes of animals having this transgene contained 35.7 ± 7.5 type II NBs and many INPs (Fig. 9J,N). The heterozygosity of *brm* or *mor* enhanced the supernumerary NB phenotype in $numb^{NP2301/15}$ brains (Fig. 9K-L) (Janssens & Komori et al. 2014).

Since Erm as well as the BAF complex function temporally after Brat and Numb in immature INPs to suppress supernumerary NB formation it was tested whether Erm and the BAF complex might function synergistically to restrict the developmental potential in immature INPs. Both heterozygosity of *erm* and reduced BAF complex enhanced the supernumerary NB phenotype in $numb^{NP2301/15}$ brains (Fig. 9M-N). Most importantly, while over-expression of the $UAS\text{-}brm^{DN}$ transgene alone did not have any effect on the type II NB lineage, over-expression of brm^{DN} significantly increased the formation of supernumerary NB in *erm* hypomorphic brains (Fig. 9O-Q) (Janssens & Komori et al. 2014).

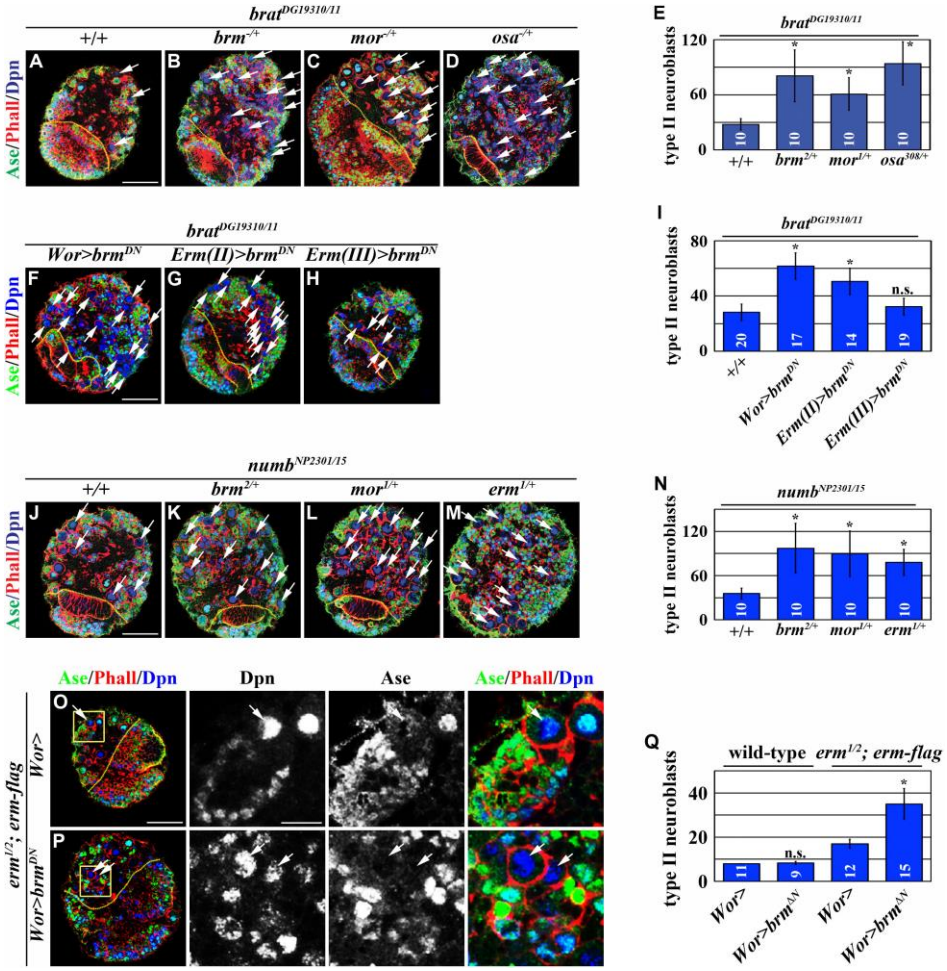

Fig 9: The BAP complex functions cooperatively with Erm to restrict the developmental potential in immature INPs (Janssens & Komori et al. 2014)

(A-E) Reduced function of the BAP complex enhances the supernumerary NB phenotype in brat hypomorphic brains. (A-D) Third instar larval brains of the indicated genotypes were stained for the markers indicated. Scale bar, 40 µm. (E) Quantification of total type II NBs per lobe for the indicated genotypes. Numbers inside the bars indicate the number of animals used for counting. The asterisks indicate the the difference between the wt and the sample is significant while n.s. stands for non-significant.

(F-I) Reducing *brm* function in Ase- immature INPs enhances the supernumerary NB phenotype in brat hypomorphic brains. (F-H) Third instar larval brains of the indicated genotypes were stained for the markers indicated. Scale bar, 40 µm. (I) Quantification of total type II NBs per lobe for the indicated genotypes. Numbers inside the bars indicate the number of animals used for counting. The asterisks indicate the the difference between the wt and the sample is significant while n.s. stands for non-significant.

(J-N) Reduced function of the BAP complex or *erm* enhances the supernumerary NB phenotype in numb hypomorphic brains. (J-M) Third instar larval brains of the indicated genotypes were stained for the markers indicated. Scale bar, 40 µm. (N) Quantification of total type II NBs per lobe for the indicated genotypes. Numbers inside the bars indicate the number of animals used for counting. The asterisks indicate the the difference between the wt and the sample is significant while n.s. stands for non-significant.

(O-Q) Reducing *brm* function enhances the supernumerary NB phenotype in *erm* hypomorphic brains. Third instar larval brains of the indicated genotypes were stained for the markers indicated. The high magnification image of the boxed area in the low magnification image is shown below. Scale bars, 40 µm in the low magnification image and 10 µm in the high magnification image. (Q) Quantification of total type II NBs per lobe for the indicated genotypes. Numbers inside the bars indicate the number of animals used for counting. The asterisks indicate the the difference between the wt and the sample is significant while n.s. stands for non-significant.

3.4. Protocol for the isolation of specific RNA using the TU-tagging system

3.4.1. Visual observation of expression in cells

It was observed that the *UAS-UPRT* system drives expression if expressed with *Wor-Gal4* as well as *Erm(III)-Gal4*. Importantly, *Erm(III)* drove expression stronger than *wor* but there was also a stronger unspecific expression observed (Fig. 10).

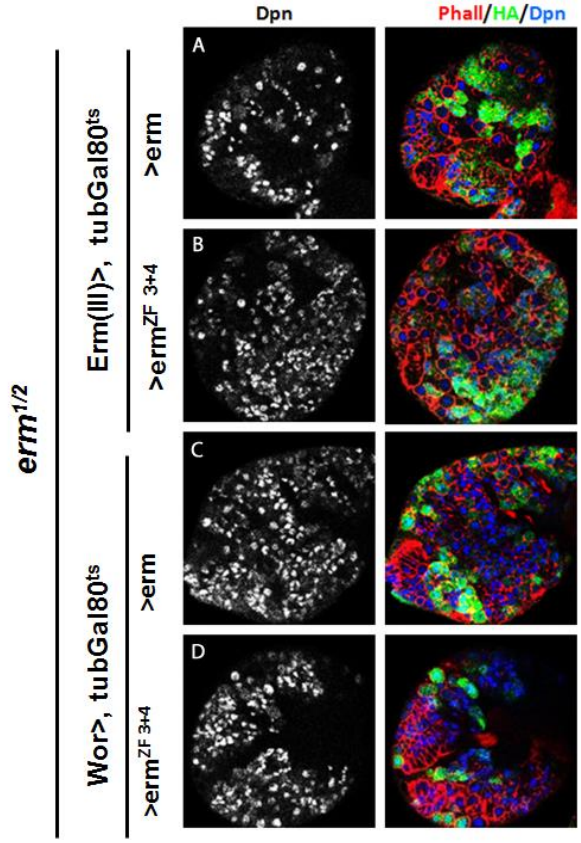

Fig 10: UPRT transgene expression in larval brains

(A-D) Third instar larval brains were stained for the markers indicated. The HA tag was on the UPRT transgene and thus the HA stain (green) shows if and where the transgene is expressing. All brains had an *erm* null background and tubGal80^{ts}.

Erm (III) was driving expression in A and B while Wor was driving expression in C and D. In A and C the expression of erm was driven and in B and D the expression of erm$^{ZF\ 3+4}$. It can be seen that there is expression in all brains.

3.4.2. Trial run

To test the TU-protocol larval brains were harvested on 3 days. ~500 brains of larvae driven by the Wor-Gal4 Ase-Gal80 combination and ~500 brains of larvae with UPRT expression driven by Ase-Gal4 were collected each day. Nanodrop readings were performed before (Tbl. 12), after RNA purification (Tbl. 13) and at the end of the protocol to control the result.

Tbl. 11: Amount of RNA before RNA purification

	Wor-Gal4 Ase-Gal80			Ase-Gal4		
	1	2	3	1	2	3
A 260/280	1.85	1.92	1.90	1.85	1.72	1.78
Conc [ng/µl]	430.6	943.7	887	406.5	360.8	460
Volume [µl]	50	50	50	50	50	50
Total Amount [µg]	21.53	47.185	44.35	20.325	18.04	23

RNA purification was performed for all samples except Wor 2 and 3 due to already sufficient purity.

Tbl. 12: Amount of RNA after purification

	Wor-Gal4 Ase-Gal80			Ase-Gal4		
	1	2	3	1	2	3
A 260/280	2.24	1.92	1.90	2.25	2.13	2.26
Conc [ng/µl]	359.1	943.7	887	88.2	205	189.8
Volume [µl]	50	50	50	50	50	50
Total Amount [µg]	17.96	47.185	44.35	4.41	10.25	9.49

To gain a sufficient amount of RNA for the Biotinylation step half of the sample Wor 1 was added to Wor 2 and Wor 3 each while the Ase samples were all mixed together.

Tbl. 13: Final yield of RNA

	Wor-Gal4 Ase-Gal80		Ase-Gal4
	2	3	
A 260/280	1.94	1.34	2.12
Conc [ng/µl]	7.1	3.4	7.4
Volume [µl]	15	15	15
Total Amount [µg]	0.36	0.17	0.37

3.4.3. Troube shooting

To find errors in the TU-tagging protocol/procedure a few tests were conducted.

RNA samples were collected before and after biotinylation and then run on a gel to control if there was RNA degradation during one of the steps (Fig. 11).

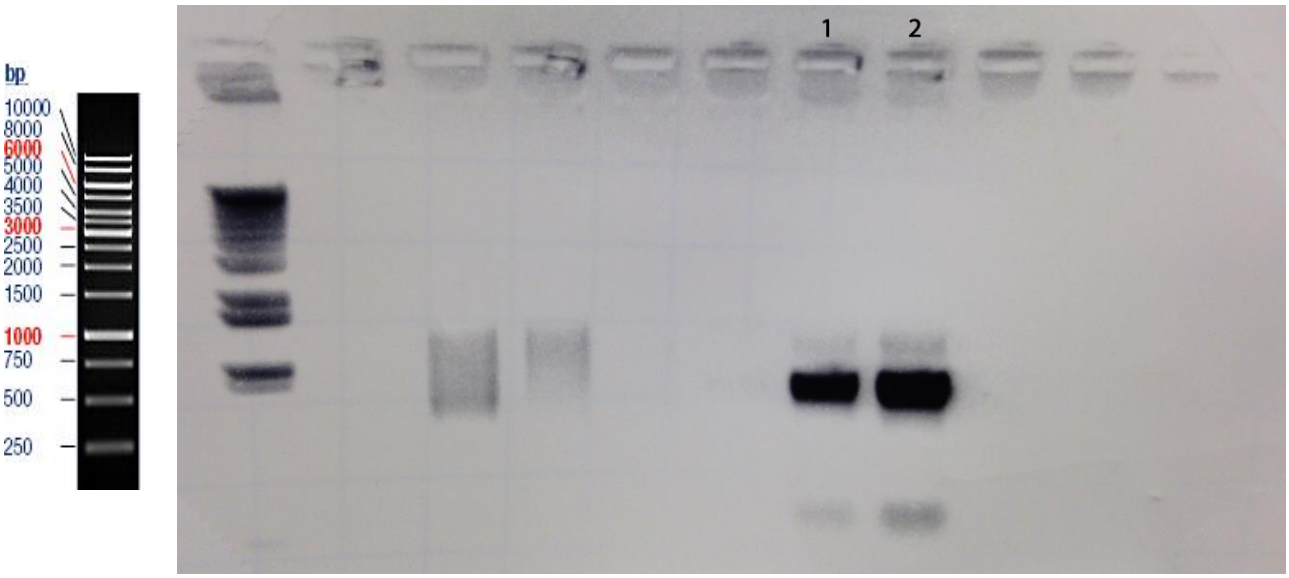

Fig 11: RNA Degradation control

To control if the RNA gets degraded during a step of the TU-tagging protocol two samples were taken, one before (1) and one after (2) the biotinylation reaction. Both samples have bands and a slight smear.

Next it was tested if there was only little or no TU-tagged RNA yield. Therefore expression was driven by hs-Gal4 to achieve a high amount of tagged RNA disregarding where it was expressed.

Since there were fly lines containing the UAS-UPRT transgene from two different labs, the Cleary lab and the O'connor lab, it was additionally tested which flies tagged RNA more efficiently. Therefore the flies from both labs were crossed to hs-Gal4 and additionally tubGal4 was crossed to the hs-Gal4 to serve as a negative control. Also since the expression levels were expected to be high but it could not be predicted exactly how high 10 and 50 whole larvae were harvested from the different fly lines each.

Tbl. 14: TubGal4 and O'connor fly lines before RNA cleanup

Purity, concentration and amount of RNA gained from the extraction of the TubGal4 and O'connor fly lines. Different amounts of larvae were used and additionally whole larvae were collected of the larvae coming from the crosses that did not have the UPRT transgene to serve as a negative control. Due to an accident some solution from the sample containing RNA of 50 larvae of the TubGal4 line was lost resulting in a much lower RNA yield.

Fly line	TubGal4		O'connor			
Brain amount	10	<50	10		50	
Presence of UPRT	-	-	+	-	+	-
A 260/280	1.79	1.66	1.75	1.70	1.75	1.75
Conc [ng/µl]	1824.2	884.8	2029.6	1357.7	4248	2434.3
Volume [µl]	50	50	50	50	50	50
Total Amount [µg]	91.21	44.24	101.48	67.89	212.40	121.72

Tbl. 15: Cleary fly lines before RNA cleanup

Purity, concentration and amount of RNA gained from the extraction of the Cleary fly line. Different amounts of brains were used and additionally larval brains were collected of the larvae coming from the crosses that did not have the UPRT transgene to serve as a negative control.

Fly line	Cleary			
Brain amount	10		50	
Presence of UPRT	+	-	+	-
A 260/280	1.79	1.76	1.86	1.80
Conc [ng/µl]	1925.2	2027	3192.3	2063.3
Volume [µl]	50	50	50	50
Total Amount [µg]	96.26	101.35	159.62	103.17

It was concluded that the amount of RNA gained from 10 larvae was sufficient and therefore the RNA cleanup was only conducted on samples containing RNA from 10 larvae (Tbl. 16).

Tbl. 16: RNA yield after RNA cleanup

Purity, concentration and amount of RNA gained after performing a RNA cleanup. 100 µl water were used to elute the RNA to gain a higher yield.

Fly line	TubGal4	O'connor		Cleary	
Presence of UPRT	-	+	-	+	-
A 260/280	2.26	2.32	2.29	2.30	2.29
Conc [ng/µl]	151.2	348.8	394.6	263.7	378.3
Volume [µl]	100	100	100	100	100
Total Amount [µg]	15.12	34.88	39.46	26.37	37.83

Unfortunately the results indicated that too little or no tagged RNA could be isolated using the developed protocol.

3.5. Protocol for the isolation of specific DNA using the TADA-system

It was observed that the used LT3-Dam is getting expressed in the brain cells (Fig 12B). However, a slight unspecific expression can be seen which could cause a background in later experiments (Fig. 12A).

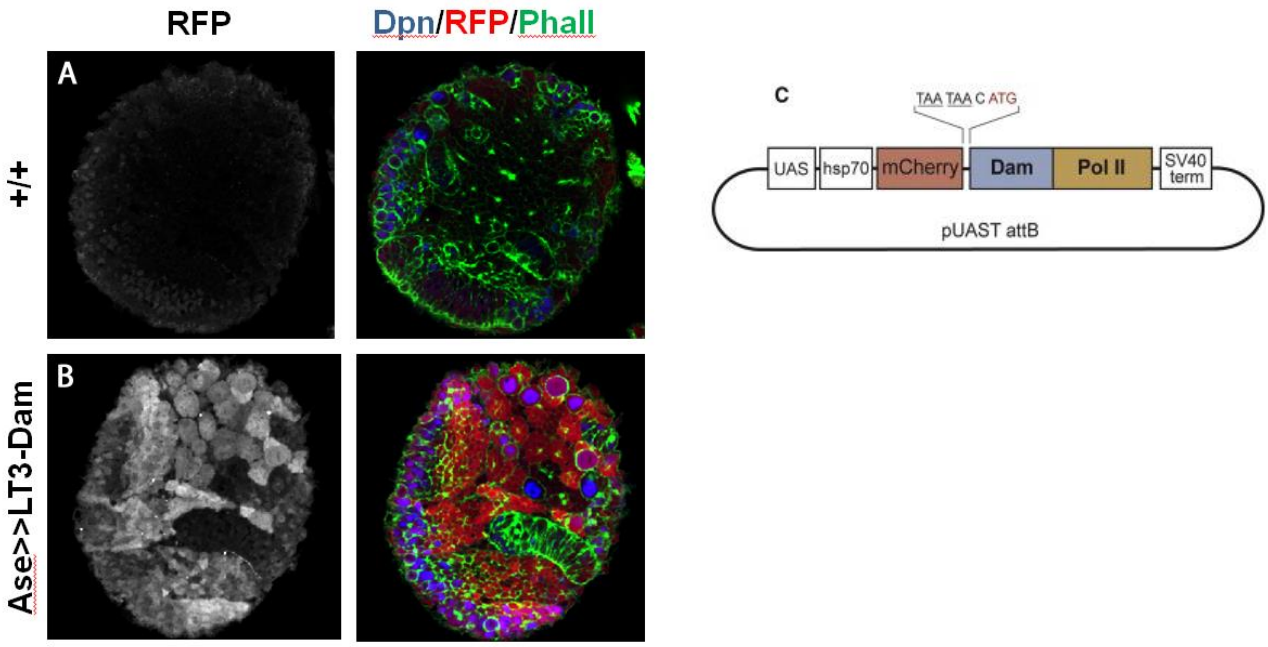

Fig 12: Expression of LT3-Dam
(A-B) Third instar larval brains were stained for the markers indicated. RFP (red) marks expression of the Dam construct. (A) A brain lobe with a wild type background as a control. Only very little RFP can be observed. (B) LT3-Dam was expressed by Ase. A very strong RFP stain can be seen which indicates a strong expression of the Dam construct.

(C) Design of the TaDa construct for profiling RNA Pol II occupancy in the genome (Southall et al., 2013).

3.5.1. First trial run

To test the designed protocol 3 different fly lines were used. The first served as a negative control and thus did not have Ase-Gal4 to drive expression and had no LT3-Dam transgene (Fig. 13.1). The second also did not have an Ase-Gal4 but it did have the LT3-Dam transgene (Fig. 13.2). The third one has got the Ase-Gal4 as well as the LT3-Dam transgene and using this fly line two additional controls were made (Fig. 13.3). For one no DpnI enzyme was used for the DpnI digestion (Fig. 13.4) and for the other one no T4 quick ligase was used for the ligation step (Fig. 13.5).

Expression was induced by shifting the larvae to 31°C for 24 hrs.

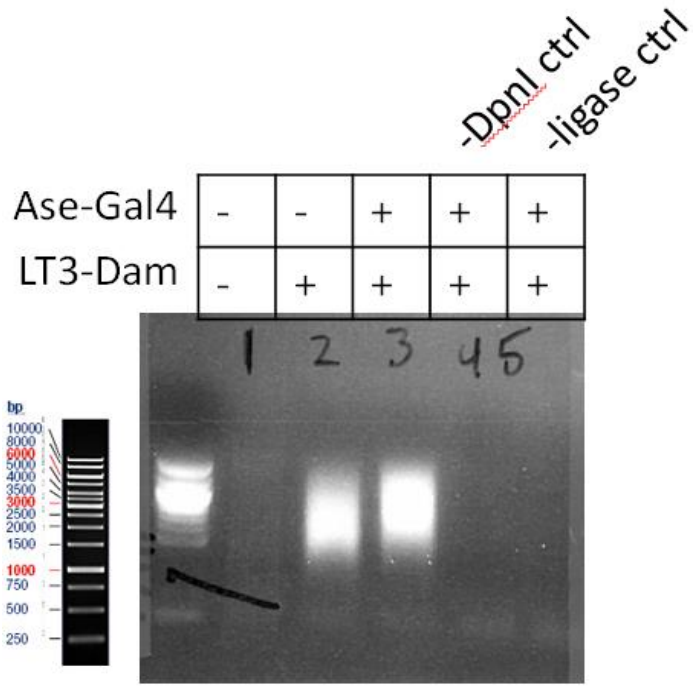

Fig 13: Results of the first trial run of the TADA protocol
A 1 % agarose gel with a 1 kb ladder loaded in the first line. The table above shows which transgenes the lines below had. A strong smear can be observed in the samples 2 (Ase-Gal4 -,LT3-Dam +) and 3 (Ase-Gal4^{+},LT3-Dam^{+}) . Sample 1 (Ase-Gal4^{-},LT3-Dam^{-}) got a very slight smear and in samples 4 (Ase-Gal4^{+},LT3-Dam^{+}, no DpnI digestion) and 5 (Ase-Gal4^{+},LT3-Dam^{+}, no ligation) no smear can be observed. These Results indicate that the isolation of DNA worked since there is a smear on 3 but not on 4and 5. However, also a lot of DNA is getting marked nonspecifically at the chosen conditions as there is a similar smear on 2.

3.5.2. Second trial run

For the second trial run samples were collected in duplicates to compare the expression levels when inducing expressions at 25°C and 29°C. The samples containing the LT3-PolII as well as the Erm-Gal4,tubgal80^{ts} transgenes had the strongest smear while the samples without the Erm-Gal4,tubgal80^{ts} had only a very slight smear (Fig. 14). The LT3-Dam (LT3-ctrl) had also a slight smear.

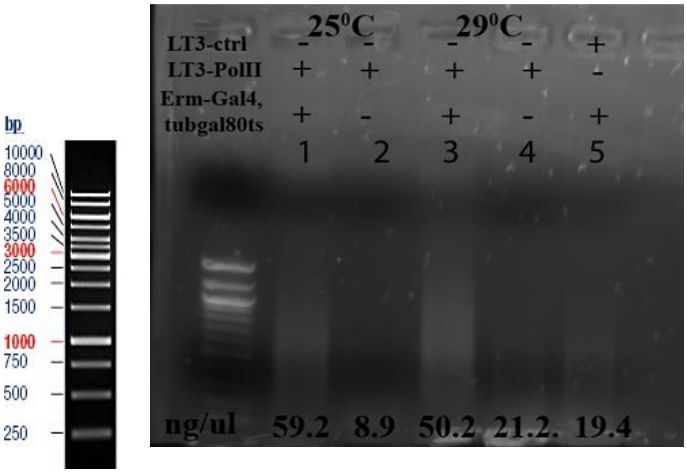

Fig 14: Results of the second trial run of the TADA protocol
A 1 % agarose gel with a 1 kb ladder loaded in the first line. At the bottom the DNA concentrations of the samples can be seen. The first two lines were loaded with the samples were expression was induced using 25°C. The last 3 lines were loaded with samples where expression was induced using 29°C. The +/- show which transgenes were in the sample loaded in the line below. Samples 1 (LT3-ctrl^{-}, LT3-PolII^{+}, Erm-Gal4,tubGal80ts^{+}) and 3 (LT3-ctrl^{-}, LT3-PolII^{+}, Erm-Gal4,tubGal80ts^{+}) got the strongest smear and the highest concentrations. There can also be a sight smear observed in samples 4 (LT3-ctrl^{-}, LT3-PolII^{+}, Erm-Gal4,tubGal80ts^{-}) and 5 (LT3-ctrl^{+}, LT3-PolII^{-}, Erm-Gal4,tubGal80ts^{+}). No smear can be seen in sample 2 (LT3-ctrl^{-}, LT3-PolII^{+}, Erm-Gal4,tubGal80ts^{-}). These results indicate that less unspecific DNA is getting marked when driving expression at 25°C than at 29°C while the total amount of isolated DNA is about the same at both conditions. LT3-ctrl is also marking DNA which could be isolated, however, at a much lower level than LT3-PolII.

3.6. CG6520 enhancer region

3.6.1. CG6520 interaction

The interaction of *CG6520* with *erm* was observed because homozygous mutation of *CG6520* significantly enhanced the *erm* hypomorphic background (Fig. 15A-B). Additionally driving expression of *CG6520* in immature INPs and INPs significantly suppressed supernumerary NB formation in an *erm* mutant background (Fig 15C-D).

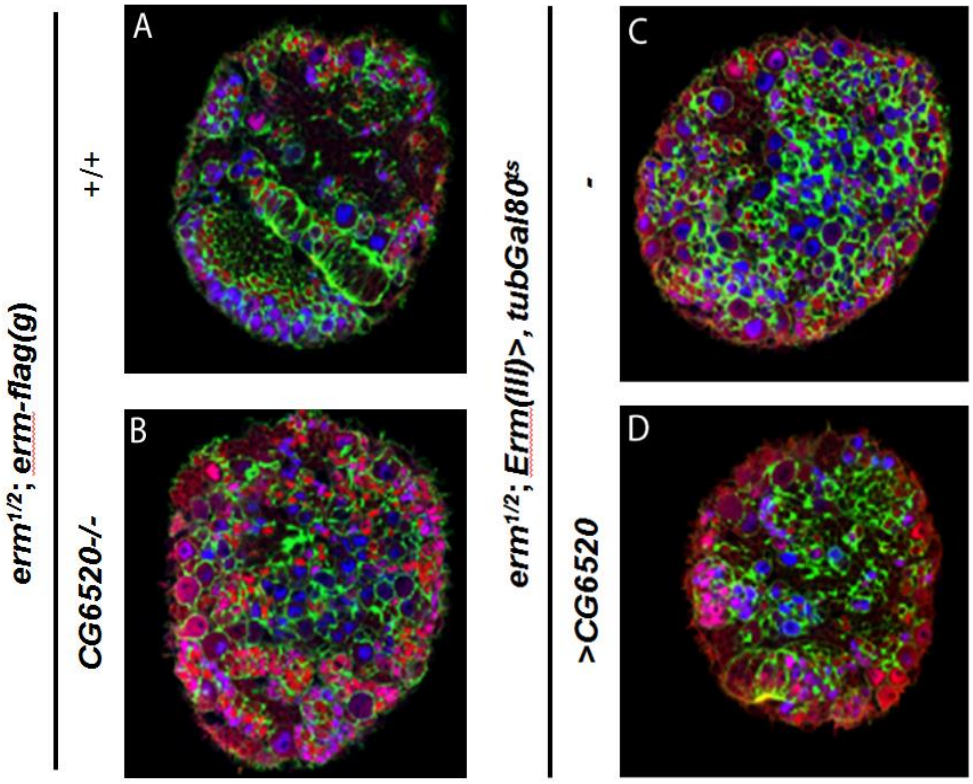

Fig 15: CG6520 genetically interacts with erm

(A-D) Third instar larval brains were stained for the markers indicated. A and B brains had an *erm* hypomorphic background. C and D are in an *erm* null mutant background.
(A-B) The larva had additionally erm-flag (g) for slight expression of erm. A is the wt control and B had a CG6520$^{-/-}$ mutation. It can be seen that A has far less ectopic NBs (Dpn^{+}, Ase^{-}) than B.
(C-D) The larva had additionally Erm (III) driving Gal4 under the control of tubGal80ts. In brain C there was no specific gene expressed while in brain D the expression of CG6520 was driven. D had far less ectopic NBs (Dpn^{+}, Ase^{-}) than C.

3.6.2. Cloning of the CG6520 enhancer region

Due to observation of genetic interaction between *erm* and *CG6520* (Fig. 15), it was decided to investigate the expression pattern of the Cg6520 gene. Therefore the *CG6520* enhancer region had to be cloned into the pBPG vector. To gain the *CG6520* enhancer region a PCR was performed using specific primers (Tbl. 17). The region was 2,190 bp long. After running the PCR product on a 1 % agarose gel the length could be controlled and then the region with the band at around 2000 bp was cut out (Fig. 16). A gel extraction was performed to prepare the PCR product for further use.

Tbl. 17: Primers for CG6520 enhancer PCR

Forward Primer	CACCAATAGACACACGACAGCTGCG
Reverse Primer	GCTTAGAGGATGATCTACTAGACTTAAGC

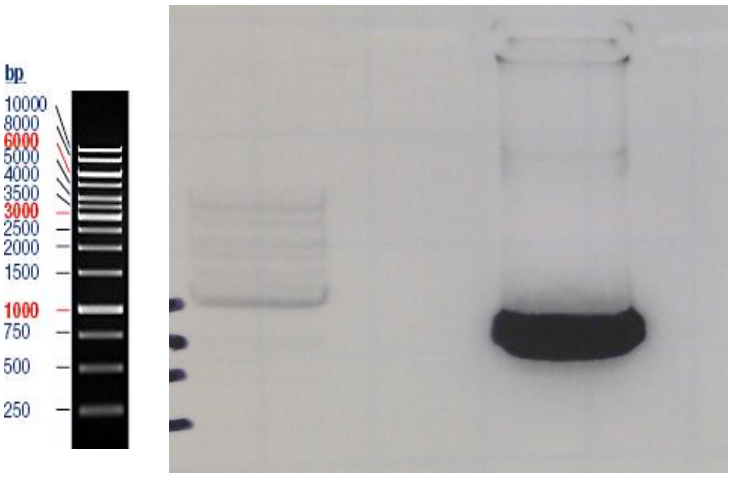

Fig 16: CG6520 enhancer region
A 1 % agarose gel with a 1 kb ladder loaded in the first line. In the second line the *CG6520* enhancer PCR product was loaded. A strong band can be seen around the 2000 bp mark suggesting that the PCR worked.

After the *CG6520* enhancer region was cloned into pENTR/D-TOPO and bacterial cultures were made, a restriction digest was performed on the plasmid of 3 chosen colonies using the NotI and PstI enzymes. The result was run on a gel to control if the cloning worked and the plasmids have the insert (Fig. 17). The total length of pENTR/D-TOPO and the insert is 4,770 bp.

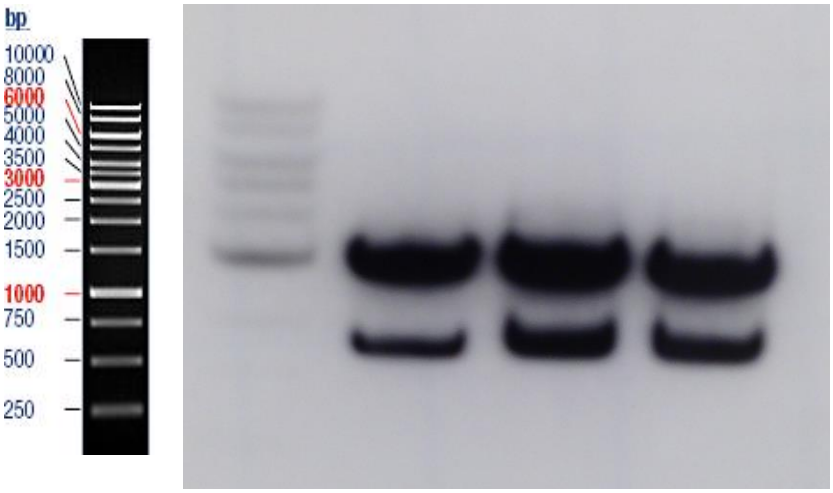

Fig 17: Result of the restriction digest
A 1 % agarose gel with a 1 kb ladder loaded in the first line. In the other lines the results of the three restriction digests were loaded. All of them have two bands, one around 3,000 bp and the other between 1,500 bp and 2,000 bp.

3.6.3. CG6520 expression pattern

The flies containing the *CG6520* enhancer region were used to observe the expression pattern of *CG6520*. CG6520 expression was visualized by driving mcD8-GFP expression by the *CG6520* promoter. This causes expression of GFP in the membrane of cells that usually express CG6520. Thereby it could be observed that CG6520 is likely expressed throughout the Type II NB linage and at lower levels in Type I NB linages (Fig. 18).

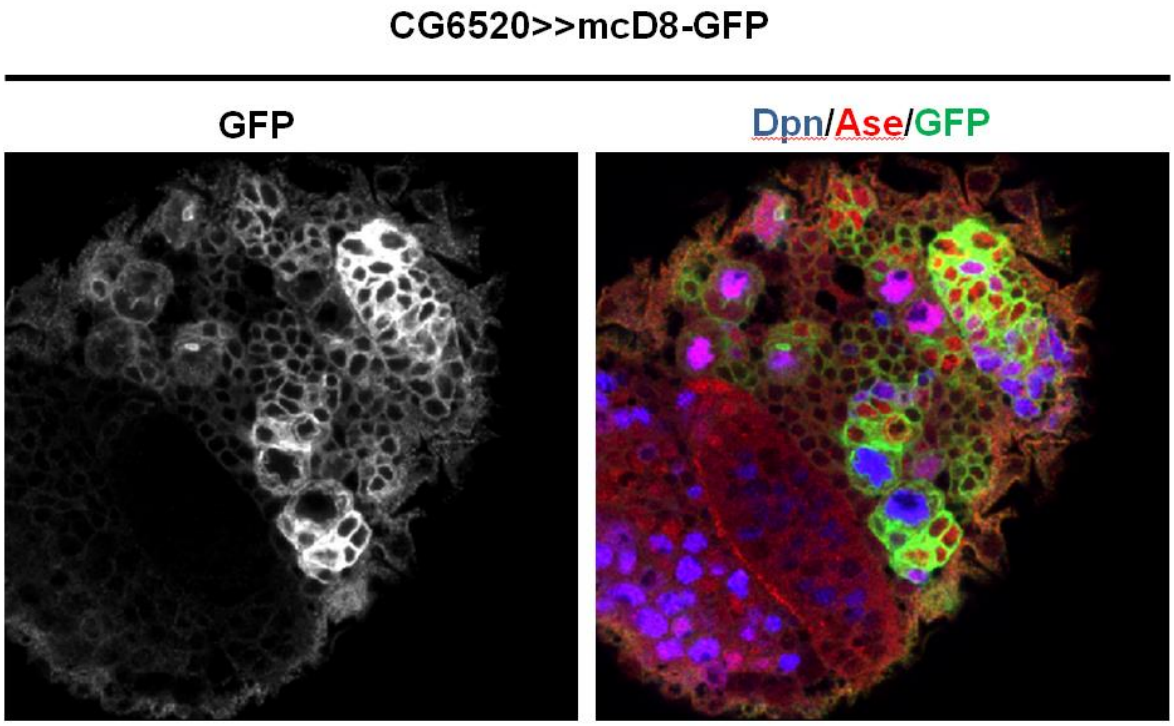

Fig 18: Expression pattern of CG6520

Third instar larval brains were stained for the markers indicated. GFP (green) was expressed in the membrane of cells which usually express CG6520 using mcD8-GFP.

4. DISCUSION

4.1. Erm-dependent restriction of the developmental potential in immature INPs leads to an attenuated competence to respond to self-renewal transcription factors in INPs

It could be observed that by removing the function of the self-renewal factors *klu, dpn* and *E(spl)mγ* the supernumerary NB phenotype caused by *erm* null brains was suppressed completely (Fig. 6-8). Therefore it is very likely that both of the genes are indispensable for supernumerary NB formation in erm null brains. Due to Erms restriction of developmental potential in immature INPs, it could be concluded that the underlying mechanism that leads to supernumerary NB formation in erm null brains is an aberrant increase in *klu, dpn* or *E(spl)mγ* expression. However, Ase^{+} immature INPs in erm null type II NB clones never showed a premature onset of Dpn expression, and over-expression of *erm* in NB did not affect Dpn expression (Weng et al., 2010). Also it was shown using transcriptome analysis that dpn and klu become up-regulated to simiar level in bratand *erm* null brains as compared to control brains (H.Komori and C.-Y.Lee, unpublished data). Thus, these data strongly suggest that it is unlikely that an aberrant increase in *dpn* or *klu* transcription leads to supernumerary NB formation in *erm* null brains (Janssens & Komori et al. 2014).

The mechanism that Erm restricts developmental potential by attenuating the competence to respond to NB self-renewal factors is more likely for the following reasons. First, the spatial and temporal expression pattern of Erm and NB self-renewal factors are non-overlapping. Second, while the over-expression of the dominant-negative VP16-Erm^{zf} or a single NB self-renewal factor alone induced a very weak supernumerary NB phenotype, co-expression of VP16-Erm^{zf} and a single NB self-renewal factor led to a very robust supernumerary NB phenotype (Fig. 6-8). Finally, while removing the function of a single NB self-renewal factor in a wt brain did not cause a change of the phenotype regarding type II NBs and their linage (Xiao et al., 2012; Zacharioudaki et al., 2012; Zhu et al., 2012), the removal of *dpn* and *klu* function alone completely suppressed the supernumerary NB phenotype in *erm* null brains (Fig. 6-8). Altogether these observations strongly suggest that stable restriction of developmental potential by the Erm-dependent mechanism in immature

INPs leads to attenuated competence to respond to the re-activation of NB self-renewal factors in INPs (Janssens & Komori et al. 2014).

4.2. Erm might function cooperatively with the BAF chromatin-remodeling complex to modify the genomic response to neuroblast self-renewal factors

The SWI/SNF ATP-dependent chromatin-remodeling protein complexes play a critical role in modifying the genomic responses to accommodate dynamic changes in the expression of transcription factors during normal development and maintenance of homeostasis (Ho & Crabtree, 2010; Narlikar, Sundaramoorthy, & Owen-Hughes, 2013; Wilson & Roberts, 2011).It was observed that by knocking down the function of several subunits in the BAP complex supernumerary NB formation is caused in larval brains using a genome-wide RNAi study (Neumüller et al., 2011). It could be independently identified that the core components of the BAF complex brm, mor and osa likely function temporally after Brat and Numb to restrict the developmental potential in the Ase^{-} immature INPs (Fig. 8). By taking into account that Brm and Osa are expressed ubiquitously in all cells in larval brains (H.Komori and C.-Y.Lee, unpublished data), it could be hypothesized that the BAP complex functions cooperatively with a transcription factor that is uniquely expressed in the immature INPs to cause its function in restricting developmental potential. The only known transcription factor uniquely expressed in immature INPs is Erm and is therefore an excellent candidate for functioning cooperatively with the BAP complex to restrict the developmental potential in the immature INPs. This hypothesis could be strengthened by showing that by reducing the function of Brm the supernumerary phenotype in erm hypomrphic brains got enhanced (Fig. 8O-Q). Therefore it is likely that Erm restricts the developmental potential in the immature INPs by recruiting the BAP complex to specific genomic loci where the BAP complex alters the nucleosome structures leading to attenuated competence to respond to the re-activation of NB self-renewal factors (Janssens & Komori et al. 2014). It will be required to perform additional functional and biochemical experiments in the future to validate this hypothesis.

4.3. TU-tagging

Using the information on the TU-tagging system (Miller et al., 2009), a protocol was developed to enable the isolation of RNA from intact larval brains. When observing the expression of the erm UPRT transgene driven by Wor or Erm(III) it could be seen that there is strong expression using both systems whereby Erm(III) seems to drive expression slightly stronger (Fig. 9A,C). However, when looking at the expression of a nonfunctional erm transgene there is also slight expression whereby Erm(III) seems to drive expression slightly stronger again (Fig. 9B,D). Thus it can be concluded that Erm(III) drives expression stronger than Wor but also has stronger nonspecific expression of TU-tagged RNA causing a stronger background. More experiments need to be conducted to find the most beneficial conditions at which very high expression of tagged RNA of erm is gained at a very low background. The main conditions to look into are the temperature and the amount of time at which expression is induced.

To test the developed protocol a trial run was conducted using 2 different fly strains with ~1500 larval brains each. The result indicated that no tagged RNA could be isolated using the protocol as the measured amount of RNA is too low to determine if the measured amount is real (Tbl. 14). Also if it were real the amount of isolated RNA would be still too low to be used for further steps. Thus the amount of larva brains needed would require an unreasonable amount of work.

Therefore it was decided to conduct some experiments to find errors in the protocol so that the amount of isolated RNA can be improved. First it was controlled if RNA degradation due to an unclean work environment caused loss of RNA. The two samples run on a gel both shoed a smear indicating that neither before nor after the biotinylation reaction step RNA degradation occurred (Fig. 10). Thus it was concluded that the cleanliness of the workspace was sufficient. Next to control if any RNA could be isolated at all fly strains with expression systems driving in a lot more cells were chosen. Additionally fly strains containing the UPRT transgene were taken from two different labs to test which one works better. However, no isolated RNA could be measured at the end indicating that using the developed protocol does not isolate any tagged RNA at all as there should have been a lot more TU-tagged RNA than in the first trial run.

As the protocol was developed using the TU-tagging protocol of the Miller lab, which already worked to isolate RNA (Miller et al., 2009), it should not be necessary to completely discard the protocol. Therefore it should be sufficient to make some changes in the protocol and conduct further experiments in the future to find out where the errors occur.

4.4. TADA-system

Since the TU-tagging protocol did not work it was decided to try a different approach which uses the TADA-system (Southall et al., 2013).

It was confirmed that the LT3-Dam construct is strongly expressing in the cells and can be used for further experiments as there is a strong stain caused by RFP which was used to mark LT3-Dam expression (Fig. 12).

In the first trial run where expression was driven at 31°C for 24 hrs. it was observed that the double negative control as well as the DpnI control and the ligase control did not have isolated DNA after running them through the developed protocol. The sample containing the LT3-Dam construct and the expression system did show isolated DNA. However, the sample having LT3-Dam but lacking the expression system also had a similar amount of isolated DNA. These results indicate that the protocol is sufficient in isolating the wanted DNA but the chosen conditions drive expression so strong that also a lot of nonspecific DNA gets marked (Fig. 13).

Therefore in the second trial run expression was driven at two lower temperatures to reduce the expression level and thus the unwanted background. The results showed that the best temperature for driving expression is 25°C as the concentration of isolated DNA was similar to expression at 29°C but the amount of the background was much lower. However, the amount of isolated DNA of the LT3-Dam construct was quite low at 29°C and thus expression driven at 25°C might result in too little DNA being expressed for further use (Fig. 14). Consequently it is necessary to conduct more experiments to improve the protocol so that a sufficient amount of wanted isolated DNA is gained at a lower background.

4.5. CG6520 plays a role in the self-renewal network

The cloning of the *CG6520* enhancer region was a success and the resulting clones were sent to the company Bestgene to create flies containing the enhancer region. Using these flies further experiments could be conducted to investigate the function of *CG6520*.

It was observed that when removing the function of *CG6520* in an *erm* hypomorphic brain the supernumerary NB phenotype gets enhanced (Fig 15A-B). This is evidence that *CG6520* plays a role in suppressing self-renewal in Type II NB linages. Additionally when overexpressing *CG6520* in an *erm* null brain the supernumerary NB phenotype gets suppressed strengthening the hypothesis that *CG6520* is self-renewal suppressor and indicating that *CG6520* somehow interacts with *erm* to control self-renewal (Fig. 15C-D). Furthermore it was observed that *CG6520* gets expressed throughout the whole Type II cell linage suggesting that it needs to interact with other genes to suppress self-renewal (Fig. 18). Further experiments are necessary to investigate the interactions of *CG6520* with other parts of the self-renewal network and its functions.

5. CONCLUSION

It was successfully shown that Erm functions in the Ase- and Ase+ immature INPs to restrict their genomic response to NB self-renewal factors which leads to a repressed competence to response to these factors in INPs. Furthermore it was identified that the BAP chromatin-remodeling complex functions together with Erm in immature INPs to suppress the formation of supernumerary NBs. Therefore it is proposed that Erm functions cooperatively with the BAP complex to implement a stable restriction of the developmental potential in immature INPs by modifying their genome, which leads to an attenuated response to all NB self-renewal factors in INPs (Janssens & Komori et al. 2014).

The developed protocol using TU-tagging did not reach its goal as no sufficient amount of product could be gained. Further investigation is necessary to identify and correct the protocols errors.

The alternatively established protocol using the TADA-system delivered promising results and should be usable to isolate the desired product. However, further testing

needs to be conducted to improve the protocol and make sure that a sufficient amount of product is gained.

The cloning of the CG6520 promoter region was a success and could be used to investigate functions and interactions of CG6520. Thereby evidence was gained indicating that CG6520 suppresses self-renewal and might act together with Erm to accomplish this. Further studies will be needed to investigate the interactions and functions of CG6520.

6. REFERENCES

Bello, B. C., Izergina, N., Caussinus, E., & Reichert, H. (2008). Amplification of neural stem cell proliferation by intermediate progenitor cells in Drosophila brain development. *Neural development*, *3*, 5. doi:10.1186/1749-8104-3-5

Bianchi-Frias, D., Orian, A., Delrow, J. J., Vazquez, J., Rosales-Nieves, A. E., & Parkhurst, S. M. (2004). Hairy transcriptional repression targets and cofactor recruitment in Drosophila. *PLoS biology*, *2*(7), E178. doi:10.1371/journal.pbio.0020178

Bowman, S. K., Rolland, V., Betschinger, J., Kinsey, K. A., Emery, G., & Knoblich, J. A. (2008). The tumor suppressors Brat and Numb regulate transit-amplifying neuroblast lineages in Drosophila. *Developmental cell*, *14*(4), 535–46. doi:10.1016/j.devcel.2008.03.004

Brand, A. H., & Perrimon, N. (1993). Targeted gene expression as a means of altering cell fates and generating dominant phenotypes. *Development (Cambridge, England)*, *118*(2), 401–15. Retrieved from http://www.ncbi.nlm.nih.gov/pubmed/8223268

Bushman, W., Thompson, J. F., Vargas, L., & Landy, A. (1985). Control of directionality in lambda site specific recombination. *Science (New York, N.Y.)*, *230*(4728), 906–11. Retrieved from http://www.pubmedcentral.nih.gov/articlerender.fcgi?artid=1978455&tool=pmcentrez&rendertype=abstract

Carrera, I., Zavadil, J., & Treisman, J. E. (2008). Two subunits specific to the PBAP chromatin remodeling complex have distinct and redundant functions during drosophila development. *Molecular and cellular biology*, *28*(17), 5238–50. doi:10.1128/MCB.00747-08

Chang, K. C., Wang, C., & Wang, H. (2012). Balancing self-renewal and differentiation by asymmetric division: insights from brain tumor suppressors in Drosophila neural stem cells. *BioEssays : news and reviews in molecular, cellular and developmental biology*, *34*(4), 301–10. doi:10.1002/bies.201100090

Choksi, S. P., Southall, T. D., Bossing, T., Edoff, K., de Wit, E., Fischer, B. E., … Brand, A. H. (2006). Prospero acts as a binary switch between self-renewal and differentiation in Drosophila neural stem cells. *Developmental cell*, *11*(6), 775–89. doi:10.1016/j.devcel.2006.09.015

Cleary, M. D., Meiering, C. D., Jan, E., Guymon, R., & Boothroyd, J. C. (2005). Biosynthetic labeling of RNA with uracil phosphoribosyltransferase allows cell-specific microarray analysis of mRNA synthesis and decay. *Nature biotechnology*, *23*(2), 232–7. doi:10.1038/nbt1061

Daul, A. L., Komori, H., & Lee, C.-Y. (2010). Immunofluorescent staining of Drosophila larval brain tissue. *Cold Spring Harbor protocols*, *2010*(7), pdb.prot5460. doi:10.1101/pdb.prot5460

Franco, S. J., & Müller, U. (2013). Shaping our minds: stem and progenitor cell diversity in the mammalian neocortex. *Neuron*, *77*(1), 19–34. doi:10.1016/j.neuron.2012.12.022

Gay, L., Miller, M. R., Ventura, P. B., Devasthali, V., Vue, Z., Thompson, H. L., … Doe, C. Q. (2013). Mouse TU tagging: a chemical/genetic intersectional method for purifying cell type-specific nascent RNA. *Genes & development*, *27*(1), 98–115. doi:10.1101/gad.205278.112

Giniger, E., Varnum, S. M., & Ptashne, M. (1985). Specific DNA binding of GAL4, a positive regulatory protein of yeast. *Cell*, *40*(4), 767–74. Retrieved from http://www.ncbi.nlm.nih.gov/pubmed/3886158

Golic, K. G., & Lindquist, S. (1989). The FLP recombinase of yeast catalyzes site-specific recombination in the Drosophila genome. *Cell*, *59*(3), 499–509. Retrieved from http://www.ncbi.nlm.nih.gov/pubmed/2509077

Guarante, L., Roberts, T. M., & Ptashne, M. (1992). A technique for expressing eukaryotic genes in bacteria. 1980. *Biotechnology (Reading, Mass.)*, *24*, 261–3. Retrieved from http://www.ncbi.nlm.nih.gov/pubmed/1422022

Haenfler, J. M., Kuang, C., & Lee, C.-Y. (2012). Cortical aPKC kinase activity distinguishes neural stem cells from progenitor cells by ensuring asymmetric segregation of Numb. *Developmental biology*, *365*(1), 219–28. doi:10.1016/j.ydbio.2012.02.027

Hartley, J. L., Temple, G. F., & Brasch, M. A. (2000). DNA cloning using in vitro site-specific recombination. *Genome research*, *10*(11), 1788–95. Retrieved from http://www.pubmedcentral.nih.gov/articlerender.fcgi?artid=310948&tool=pmcentrez&rendertype=abstract

Hirata, T., Nakazawa, M., Muraoka, O., Nakayama, R., Suda, Y., & Hibi, M. (2006). Zinc-finger genes Fez and Fez-like function in the establishment of diencephalon subdivisions. *Development (Cambridge, England)*, *133*(20), 3993–4004. doi:10.1242/dev.02585

Ho, L., & Crabtree, G. R. (2010). Chromatin remodelling during development. *Nature*, *463*(7280), 474–84. doi:10.1038/nature08911

Homem, C. C. F., & Knoblich, J. A. (2012). Drosophila neuroblasts: a model for stem cell biology. *Development (Cambridge, England)*, *139*(23), 4297–310. doi:10.1242/dev.080515

Janssens, D. H., Komori, H., Grbac, D., Chen, K., Koe, C. T., Wang, H., & Lee, C.-Y. (2014). Earmuff restricts progenitor cell potential by attenuating the competence to respond to self-renewal factors. *Development (Cambridge, England)*, *141*(5), 1036–46. doi:10.1242/dev.106534

Kaspar, M., Schneider, M., Chia, W., & Klein, T. (2008). Klumpfuss is involved in the determination of sensory organ precursors in Drosophila. *Developmental biology*, *324*(2), 177–91. doi:10.1016/j.ydbio.2008.08.031

Komori, H., Xiao, Q., McCartney, B. M., & Lee, C.-Y. (2014). Brain tumor specifies intermediate progenitor cell identity by attenuating β-catenin/Armadillo activity. *Development (Cambridge, England)*, *141*(1), 51–62. doi:10.1242/dev.099382

Landy, A. (1989). Dynamic, structural, and regulatory aspects of lambda site-specific recombination. *Annual review of biochemistry*, *58*, 913–49. doi:10.1146/annurev.bi.58.070189.004405

Lee, C.-Y., Robinson, K. J., & Doe, C. Q. (2006). Lgl, Pins and aPKC regulate neuroblast self-renewal versus differentiation. *Nature*, *439*(7076), 594–8. doi:10.1038/nature04299

Lee, C.-Y., Wilkinson, B. D., Siegrist, S. E., Wharton, R. P., & Doe, C. Q. (2006). Brat is a Miranda cargo protein that promotes neuronal differentiation and inhibits neuroblast self-renewal. *Developmental cell*, *10*(4), 441–9. doi:10.1016/j.devcel.2006.01.017

Lee, T., & Luo, L. (1999). Mosaic analysis with a repressible cell marker for studies of gene function in neuronal morphogenesis. *Neuron*, *22*(3), 451–61. Retrieved from http://www.ncbi.nlm.nih.gov/pubmed/10197526

Lee, T., & Luo, L. (2001). Mosaic analysis with a repressible cell marker (MARCM) for Drosophila neural development. *Trends in neurosciences*, *24*(5), 251–4. Retrieved from http://www.ncbi.nlm.nih.gov/pubmed/11311363

Liang, X., Peng, L., Baek, C.-H., & Katzen, F. (2013). Single step BP/LR combined Gateway reactions. *BioTechniques*, *55*(5), 265–8. doi:10.2144/000114101

Liu, C., Sage, J. C., Miller, M. R., Verhaak, R. G. W., Hippenmeyer, S., Vogel, H., … Zong, H. (2011). Mosaic analysis with double markers reveals tumor cell of origin in glioma. *Cell*, *146*(2), 209–21. doi:10.1016/j.cell.2011.06.014

Lui, J. H., Hansen, D. V, & Kriegstein, A. R. (2011). Development and evolution of the human neocortex. *Cell*, *146*(1), 18–36. doi:10.1016/j.cell.2011.06.030

Ma, J., & Ptashne, M. (1987). The carboxy-terminal 30 amino acids of GAL4 are recognized by GAL80. *Cell*, *50*(1), 137–42. Retrieved from http://www.ncbi.nlm.nih.gov/pubmed/3297349

McGuire, S. E., Le, P. T., Osborn, A. J., Matsumoto, K., & Davis, R. L. (2003). Spatiotemporal rescue of memory dysfunction in Drosophila. *Science (New York, N.Y.)*, *302*(5651), 1765–8. doi:10.1126/science.1089035

Miller, M. R., Robinson, K. J., Cleary, M. D., & Doe, C. Q. (2009). TU-tagging: cell type-specific RNA isolation from intact complex tissues. *Nature methods*, *6*(6), 439–41. doi:10.1038/nmeth.1329

Ming, G.-L., & Song, H. (2011). Adult neurogenesis in the mammalian brain: significant answers and significant questions. *Neuron*, *70*(4), 687–702. doi:10.1016/j.neuron.2011.05.001

Mohrmann, L., Langenberg, K., Krijgsveld, J., Kal, A. J., Heck, A. J. R., & Verrijzer, C. P. (2004). Differential targeting of two distinct SWI/SNF-related Drosophila chromatin-remodeling complexes. *Molecular and cellular biology*, *24*(8), 3077–88. Retrieved from http://www.pubmedcentral.nih.gov/articlerender.fcgi?artid=381637&tool=pmcentrez&rendertype=abstract

Narlikar, G. J., Sundaramoorthy, R., & Owen-Hughes, T. (2013). Mechanisms and functions of ATP-dependent chromatin-remodeling enzymes. *Cell*, *154*(3), 490–503. doi:10.1016/j.cell.2013.07.011

Neumüller, R. A., Richter, C., Fischer, A., Novatchkova, M., Neumüller, K. G., & Knoblich, J. A. (2011). Genome-wide analysis of self-renewal in Drosophila neural stem cells by transgenic RNAi. *Cell stem cell*, *8*(5), 580–93. doi:10.1016/j.stem.2011.02.022

Pfeiffer, B. D., Jenett, A., Hammonds, A. S., Ngo, T.-T. B., Misra, S., Murphy, C., … Rubin, G. M. (2008). Tools for neuroanatomy and neurogenetics in Drosophila. *Proceedings of the National Academy of Sciences of the United States of America*, *105*(28), 9715–20. doi:10.1073/pnas.0803697105

San-Juán, B. P., & Baonza, A. (2011). The bHLH factor deadpan is a direct target of Notch signaling and regulates neuroblast self-renewal in Drosophila. *Developmental biology*, *352*(1), 70–82. doi:10.1016/j.ydbio.2011.01.019

Schwitalla, S., Fingerle, A. A., Cammareri, P., Nebelsiek, T., Göktuna, S. I., Ziegler, P. K., … Greten, F. R. (2013). Intestinal tumorigenesis initiated by dedifferentiation and acquisition of stem-cell-like properties. *Cell*, *152*(1-2), 25–38. doi:10.1016/j.cell.2012.12.012

Shaner, N. C., Campbell, R. E., Steinbach, P. A., Giepmans, B. N. G., Palmer, A. E., & Tsien, R. Y. (2004). Improved monomeric red, orange and yellow fluorescent proteins derived from Discosoma sp. red fluorescent protein. *Nature biotechnology*, *22*(12), 1567–72. doi:10.1038/nbt1037

Southall, T. D., Gold, K. S., Egger, B., Davidson, C. M., Caygill, E. E., Marshall, O. J., & Brand, A. H. (2013). Cell-type-specific profiling of gene expression and chromatin binding without cell isolation: assaying RNA Pol II occupancy in neural stem cells. *Developmental cell*, *26*(1), 101–12. doi:10.1016/j.devcel.2013.05.020

Van Steensel, B., Delrow, J., & Henikoff, S. (2001). Chromatin profiling using targeted DNA adenine methyltransferase. *Nature genetics*, *27*(3), 304–8. doi:10.1038/85871

Van Steensel, B., & Henikoff, S. (2000). Identification of in vivo DNA targets of chromatin proteins using tethered dam methyltransferase. *Nature biotechnology*, *18*(4), 424–8. doi:10.1038/74487

Vogel, M. J., Peric-Hupkes, D., & van Steensel, B. (2007). Detection of in vivo protein-DNA interactions using DamID in mammalian cells. *Nature protocols*, *2*(6), 1467–78. doi:10.1038/nprot.2007.148

Wallace, K., Liu, T. H., & Vaessin, H. (2000). The pan-neural bHLH proteins DEADPAN and ASENSE regulate mitotic activity and cdk inhibitor dacapo expression in the Drosophila larval optic lobes. *Genesis (New York, N.Y. : 2000)*, *26*(1), 77–85. Retrieved from http://www.ncbi.nlm.nih.gov/pubmed/10660675

Weisberg, R. A., Enquist, L. W., Foeller, C., & Landy, A. (1983). Role for DNA homology in site-specific recombination. The isolation and characterization of a site affinity mutant of coliphage lambda. *Journal of molecular biology*, *170*(2), 319–42. Retrieved from http://www.ncbi.nlm.nih.gov/pubmed/6226804

Weng, M., Golden, K. L., & Lee, C.-Y. (2010). dFezf/Earmuff maintains the restricted developmental potential of intermediate neural progenitors in Drosophila. *Developmental cell*, *18*(1), 126–35. doi:10.1016/j.devcel.2009.12.007

Weng, M., Komori, H., & Lee, C.-Y. (2012). Identification of neural stem cells in the Drosophila larval brain. *Methods in molecular biology (Clifton, N.J.)*, *879*, 39–46. doi:10.1007/978-1-61779-815-3_3

Weng, M., & Lee, C.-Y. (2011). Keeping neural progenitor cells on a short leash during Drosophila neurogenesis. *Current opinion in neurobiology*, *21*(1), 36–42. doi:10.1016/j.conb.2010.09.005

Wilson, B. G., & Roberts, C. W. M. (2011). SWI/SNF nucleosome remodellers and cancer. *Nature reviews. Cancer*, *11*(7), 481–92. doi:10.1038/nrc3068

Wu, J. S., & Luo, L. (2006). A protocol for mosaic analysis with a repressible cell marker (MARCM) in Drosophila. *Nature protocols*, *1*(6), 2583–9. doi:10.1038/nprot.2006.320

Xiao, Q., Komori, H., & Lee, C.-Y. (2012). klumpfuss distinguishes stem cells from progenitor cells during asymmetric neuroblast division. *Development (Cambridge, England)*, *139*(15), 2670–80. doi:10.1242/dev.081687

Yang, N., Dong, Z., & Guo, S. (2012). Fezf2 regulates multilineage neuronal differentiation through activating basic helix-loop-helix and homeodomain genes in the zebrafish ventral forebrain. *The Journal of neuroscience : the official journal of the Society for Neuroscience*, *32*(32), 10940–8. doi:10.1523/JNEUROSCI.2216-12.2012

Younger-Shepherd, S., Vaessin, H., Bier, E., Jan, L. Y., & Jan, Y. N. (1992). deadpan, an essential pan-neural gene encoding an HLH protein, acts as a denominator in Drosophila sex determination. *Cell*, *70*(6), 911–22. Retrieved from http://www.ncbi.nlm.nih.gov/pubmed/1525829

Zacharioudaki, E., Magadi, S. S., & Delidakis, C. (2012). bHLH-O proteins are crucial for Drosophila neuroblast self-renewal and mediate Notch-induced overproliferation. *Development (Cambridge, England)*, *139*(7), 1258–69. doi:10.1242/dev.071779

Zeidler, M. P., Tan, C., Bellaiche, Y., Cherry, S., Häder, S., Gayko, U., & Perrimon, N. (2004). Temperature-sensitive control of protein activity by conditionally splicing inteins. *Nature biotechnology*, *22*(7), 871–6. doi:10.1038/nbt979

Zhu, S., Wildonger, J., Barshow, S., Younger, S., Huang, Y., & Lee, T. (2012). The bHLH repressor Deadpan regulates the self-renewal and specification of Drosophila larval neural stem cells independently of Notch. (J. C. Zheng, Ed.)*PloS one*, *7*(10), e46724. doi:10.1371/journal.pone.0046724